MRI-guidance for motion management in external beam radiotherapy: current status and future challenges

C Paganelli[1,9,10], B Whelan[2], M Peroni[3], P Summers[4], M Fast[5], T van de Lindt[5], J McClelland[6], B Eiben[6], P Keall[2], T Lomax[3], M Riboldi[7] and G Baroni[1,8,10]

[1] Dipartimento di Elettronica, Informazione e Bioingegneria, Politecnico di Milano, Milano, Italy
[2] ACRF Image X Institute, Sydney Medical School, University of Sydney, Sydney, Australia
[3] Proton Therapy Center, Paul Scherrer Institute, PSI Villigen, Switzerland
[4] Divisione di Radiologia, Istituto Europeo di Oncologia IRCCS, Milano, Italy
[5] Department of Radiation Oncology, Netherlands Cancer Institute, Amsterdam, Netherlands
[6] Centre for Medical Image Computing, University College London, London, United Kingdom
[7] Department of Medical Physics, Ludwig-Maximilians-Universität München, Munich, Germany
[8] Bioengineering Unit, Centro Nazionale di Adroterapia Oncologica, Pavia, Italy
[9] Author to whom any correspondence should be addressed.
[10] www.cartcas.polimi.it

E-mail: chiara.paganelli@polimi.it

Keywords: MRI-guidance, time-resolved MRI, 4D MRI, external beam radiotherapy, organ motion management

RECEIVED 15 January 2018
ACCEPTED FOR PUBLICATION 26 October 2018
REVISED 27 September 2018
PUBLISHED 20 November 2018

Abstract

High precision conformal radiotherapy requires sophisticated imaging techniques to aid in target localisation for planning and treatment, particularly when organ motion due to respiration is involved. X-ray based imaging is a well-established standard for radiotherapy treatments. Over the last few years, the ability of magnetic resonance imaging (MRI) to provide radiation-free images with high-resolution and superb soft tissue contrast has highlighted the potential of this imaging modality for radiotherapy treatment planning and motion management. In addition, these advantageous properties motivated several recent developments towards combined MRI radiation therapy treatment units, enabling in-room MRI-guidance and treatment adaptation.

The aim of this review is to provide an overview of the state-of-the-art in MRI-based image guidance for organ motion management in external beam radiotherapy. Methodological aspects of MRI for organ motion management are reviewed and their application in treatment planning, in-room guidance and adaptive radiotherapy described. Finally, a roadmap for an optimal use of MRI-guidance is highlighted and future challenges are discussed.

1. Introduction

External beam radiotherapy is a technique in the treatment of cancer as best practice care in approximately 50% of all cancer cases (Barton *et al* 2014, Rosenblatt and Zubizarreta 2017). The goal of radiotherapy is to deliver a prescribed dose to oncologic targets, whilst minimizing the dose delivered to surrounding healthy tissues. It is well-known that motion of both tumour and nearby organs at risk introduces geometric uncertainties into this process, leading to potential underdosage of the target region, and/or overdosage in nearby organs at risk. As such, one of the most important advances in external beam radiotherapy has been the development of techniques for imaging, planning, and treatment of targets which move as a result of respiration, such as in the lung, liver, or pancreas (Keall *et al* 2006, Korreman 2012). Many technological and methodological advances were reported over the last decade, with investments in research programs, technology transfer from research to industry, and development of new generation therapy units designed to track moving targets in real-time (Keall *et al* 2006, Riboldi *et al* 2012, Kubiak 2016, Caillet *et al* 2017, Chang *et al* 2017).

The increased confidence in tumour localization enabled by these techniques paved the way for highly conformal and dose escalated treatments, such as hypo-fractionated photon treatments and particle therapy

(Kubiak 2016, Schwarz *et al* 2017). Strategies to compensate and account for motion such as breath-hold, gating or tumour tracking can be adopted (Keall *et al* 2006, Kubiak 2016), with the support of imaging techniques to accurately guide the treatment and perform adaptive image-guided radiotherapy by means of daily monitoring of anatomo-pathological changes (Dawson and Sharpe 2006, Verellen *et al* 2008, Connell and Hellman 2009, Høyer *et al* 2011, Jaffray 2012). To enable the targeting of the tumour under free-breathing conditions, the com-bination of 4D imaging for treatment planning and in-room image-guided strategies is beneficial in both photon (Keall *et al* 2006, Caillet *et al* 2017) and particle therapy (Riboldi *et al* 2012, Kubiak 2016). The rapid diffusion of 4D imaging into the clinic (Simpson *et al* 2009) and the clinical evidence and perspectives of image guidance (Verellen *et al* 2008) indicate the relevance of such a technology.

Despite these advances, standard x-ray imaging suffers from a number of shortcomings. Above all, poor soft tissue contrast makes it difficult to distinguish the tumour from the surrounding tissues. In order to overcome this, fiducial markers may be surgically implanted, however this is a time consuming and invasive procedure. In addition, x-ray based image guidance exposes patients to additional radiation dose, which at least in some cases may be clinically significant (Bujold *et al* 2012). At present, 4D computed tomography (4D CT) represents the standard clinical practice for organ motion management in treatment planning (Keall *et al* 2006, Chang *et al* 2017): by 2009, an estimated 44% of centres were using 4D CT, indicating an increase in update of 7% per year (Simpson *et al* 2009). This 4D imaging reflects anatomy at different time points during one or more samples of breathing, but the limited number of respiratory phases cannot be considered representative of each breathing cycle (intra-fraction variability) at every therapy fraction (inter-fraction variability) (Dhont *et al* 2018). Therefore, it has to be supported by on-board x-ray imaging to compensate for day-to-day variations, and by tumour motion surrogates for intra-fraction motion management during treatment (Caillet *et al* 2017). Among the latter, external surrogates are clinically used to reduce x-ray imaging frequency (Caillet *et al* 2017), however their reliability in terms of correlation with internal anatomy is questionable (Ruan *et al* 2008).

In light of these issues, magnetic resonance imaging (MRI) has emerged as an ideal technique for the guidance of high precision radiation therapy, which is a topic of growing research (figure 1). MRI provides exquisite soft tissue contrast, radiation-free imaging, high temporal resolution with fast sequences and functional imaging. These features highlight the potential of MRI to improve treatment accuracy and precision across the entire radiotherapy workflow, particularly in the presence of organ motion. For treatment planning, the superior soft tissue contrast of MRI can decrease organ delineation uncertainties (Schmidt and Payne 2015), whilst the dose-free nature of MRI enables multiple and extended acquisitions, accounting for cycle-to-cycle breathing variations (Kauczor and Plathow 2006, Biederer *et al* 2010, Jaffray 2012, Menten *et al* 2017). During treatment, the new generation of in-room MRI/x-ray treatment unit systems (Fallone 2014, Jaffray *et al* 2014, Keall *et al* 2014, Lagendijk *et al* 2014, Ménard and van der Heide 2014, Mutic and Dempsey 2014) allows direct imaging and both inter- and intra- fraction treatment adaptation strategies (Bainbridge *et al* 2017a, Menten *et al* 2017, Hunt *et al* 2018). The recent clinical application of hybrid MRI and treatment unit systems (Olsen *et al* 2014, Raaymakers *et al* 2017, Kashani and Olsen 2018) represents an important milestone in external beam radiotherapy, and this technology is expected to provide improved clinical outcomes and reduce toxicities as well as efficient workflows. Finally, functional MRI can enable improved treatment prediction, functionally weighted planning, and response monitoring, thereby increasing treatment personalization across the entire workflow of radiation oncology (Kauczor *et al* 2006, van der Heide *et al* 2012, Prestwich *et al* 2015, Bainbridge *et al* 2017b, Menten *et al* 2017).

This review aims to provide a comprehensive overview of developments in MRI-guidance and its application in external beam radiotherapy for organ motion management. Current MRI techniques to quantify organ motion are described and their applications in treatment planning, in-room guidance and adaptive radiotherapy reviewed. Finally, a roadmap for an optimal use of MRI-guidance and future challenges are discussed. Article searching was performed with Scopus investigating terms 'MRI-guidance in radiotherapy', 'MRI motion radiotherapy', 'organ motion in radiotherapy', 'image-guided radiotherapy'. We refined searches for specific issues with terms such as 'time-resolved MRI', '4D MRI', 'MRI-linac', 'in-room MRI', 'tumour tracking', 'motion modelling', 'functional MRI in radiotherapy' and combinations thereof. Only papers published in English between January 1997 and August 2018, were included. For details on MRI basics, readers are referred to McRob-bie *et al* (2017).

2. MRI techniques to quantify organ motion

In conventional strategies based on x-ray imaging, external surrogates represent the most widespread solution for organ motion quantification, and these have been exploited also in MRI. MR-compatible respiratory bellows (Rohlfing *et al* 2004) or optical systems can be used, and combined with audio-visual biofeedback to increase breathing reproducibility (Kim *et al* 2012, Lee *et al* 2016). However, it is well-known that external surrogates are not always representative of the internal motion (Koch *et al* 2004, Liu *et al* 2004, Ruan *et al* 2008). One of

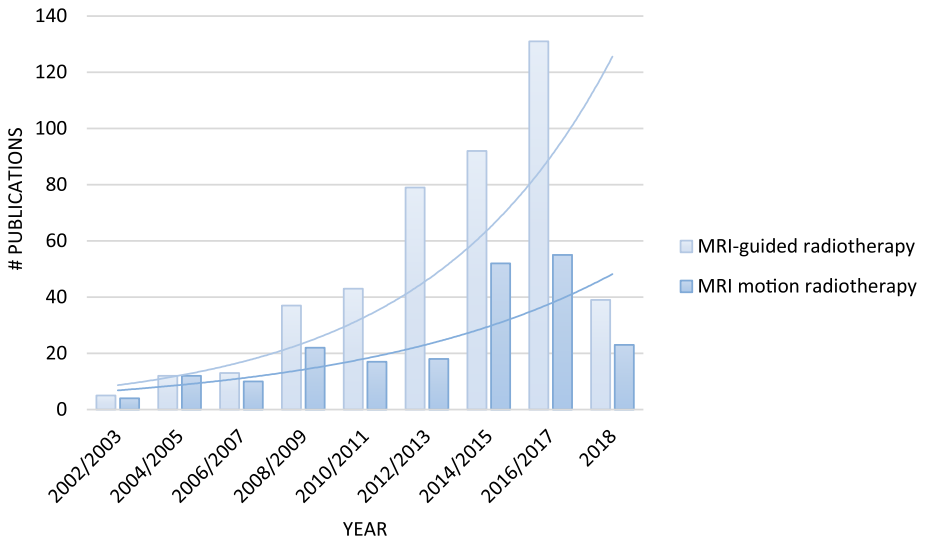

Figure 1. Trend of the publications retrieved with the search terms 'MRI-guided radiotherapy', 'MRI motion radiotherapy', from January 2002 to August 2018 (Scopus).

the main advantages of MRI is the ability to acquire the internal information over multiple respiratory cycles. At present, MRI approaches capable of resolving organ motion can be broadly classified as either time-resolved or respiratory-correlated (4D); the former delivers organ motion data in real-time at comparatively low spatial dimensionality, whilst the latter delivers comparatively high spatial dimensionality but relies on retrospective reconstruction (figure 2). Ideally, MRI for motion quantification would involve real-time 4D MRI (i.e. sub-second 3D imaging), but due to the intrinsic trade-off between spatial and temporal resolution, this is still a challenge.

2.1. Time-resolved MRI

In time-resolved MRI, image acquisition is continuously performed at sub-second frame rates (Hugo and Rosu 2012). Among time-resolved solutions, the so-called navigator echo approach entails the serial acquisition of a 1D image to map the position of the diaphragm, with a temporal resolution of up to $\approx$10 ms (Song *et al* 2011). An alternative approach is fast 2D image acquisition by means of cine-MRI, which has been described in a number of studies for respiratory motion quantification, including lung, liver, pancreas and breast (Bussels *et al* 2003, Koch *et al* 2004, Liu *et al* 2004, Plathow *et al* 2004, Rohlfing *et al* 2004, Blackall *et al* 2006, Kauczor and Plathow 2006, Kirilova *et al* 2008, Stam *et al* 2013b, Dowling *et al* 2014, Van Heijst *et al* 2016). Balanced steady state free precession MRI (bSSFP) is a form of T2/T1-weighted gradient echo (GE) imaging sequence commonly used for cine-MRI. T2-weighted turbo-spin echo (SE) sequences are an alternative to bSSFP (Kauczor *et al* 2006). Specifically, (Koch *et al* 2004) described the acquisition of fast dynamic 2D MR images with a temporal resolution of 450 ms, whereas (Plathow *et al* 2004) reported cine 2D imaging of lung cancer patients at about 300 ms. Shorter acquisition times can be achieved through the use of acceleration techniques, such as parallel imaging or reduced sampling of the *k*-space (i.e. MRI raw data) (Heidemann *et al* 2003, Pruessmann 2006, McRobbie *et al* 2017) (e.g. (Griswold *et al* 2002)), reaching approximately 150 ms (Plathow *et al* 2005, Sawant *et al* 2014). In addition, the flexibility of MRI to acquire data in arbitrary image planes allows the orientation of 2D cine-MRI along the main direction of motion (Heerkens *et al* 2014, Paganelli *et al* 2015b). Interleaved orthogonal planes (e.g. sagittal/coronal) represent a viable solution to provide pseudo-3D information of the tumour position near the slices intersection (Bjerre *et al* 2013, Tryggestad *et al* 2013b, Sawant *et al* 2014). Also for pseudo-3D acquisitions, parallel imaging techniques (Barth *et al* 2016) have been exploited to allow the acquisition of simultaneous orthogonal images (Mickevicius and Paulson 2017b), thus reducing the acquisition time and improving the respiratory motion description.

2.2. Respiratory-correlated (4D) MRI

Time-resolved 2D approaches do not enable a full 3D motion description; for this time-resolved 3D images (i.e. real-time 4D MRI) would be required. However, this is currently constrained by the limited frequency at which full 3D volumes can be acquired on the current generation of scanners (acquisition time on the order of seconds). In many approaches, the limited frequency at which full 3D volumes can be acquired requires the patient to

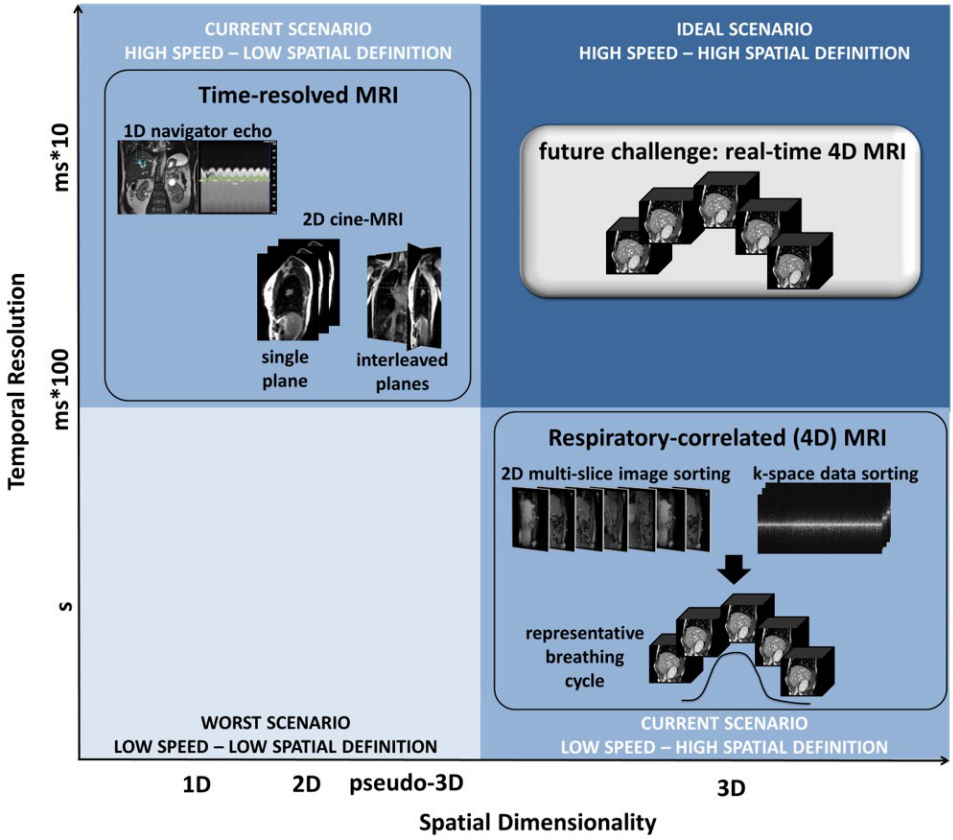

Figure 2. Image acquisition approaches in terms of temporal resolution versus spatial dimensionality. The ideal acquisition strategy would yield real-time 4D MRI; at present this is not possible and remains a future challenge.

breathe slowly or limits image quality (e.g. field of view, spatial resolution) (Blackall *et al* 2006, Plathow *et al* 2006, 2009, Dinkel *et al* 2009).

To bypass this limitation, developments have entailed 2D multi-slice cine-MRI acquisitions which are sorted and stacked into 4D MRI, deriving one representative breathing cycle like in conventional 4D CT. In the major-ity of cases, retrospective sorting is applied, although in few studies prospective gating with pre-defined bins was also reported (Tokuda *et al* 2008, Hu *et al* 2013, Du *et al* 2015, Li *et al* 2017). In retrospective methods inherited from 4D CT, sorting of slices is usually based on an external surrogate (Hu *et al* 2013). Different strategies were investigated to improve the performance of the external surrogate, either making use of audio-visual biofeed-back (To *et al* 2016) or advanced sorting (Tryggestad *et al* 2013b, Du *et al* 2015, Liu *et al* 2015, Liang *et al* 2016). As previously mentioned however, the use of internal breathing surrogates directly extracted from the acquired 2D images has been shown to increase robustness in organ motion description with respect to external surrogates (Stemkens *et al* 2015, Liu *et al* 2016a, Li *et al* 2017). Two main methods based on navigator sequences (Von Sie-benthal *et al* 2007, Tokuda *et al* 2008, Wachinger *et al* 2012) or image-derived approaches (Cai *et al* 2011, Liu *et al* 2014, 2017, Paganelli *et al* 2015c, Fontana *et al* 2016, Hui *et al* 2016, Uh *et al* 2016, van de Lindt *et al* 2018a, 2018b) are reported in the literature, relying on the acquisition of a navigator for sorting data, or on the derivation of the information directly from the data itself, respectively. These have been investigated with different image acquisi-tion schemes (e.g. cine, sequential or interleaved) (Liu *et al* 2015, 2016a) and plane orientations. Table 1 provides an overview of these methods based on prospective and retrospective image sorting. To our knowledge, a com-prehensive comparison of these approaches for the evaluation of the best solution is not available, thus limiting their application in a clinical setting. Visual biofeedback was compared against a free-breathing acquisition (To *et al* 2016), whereas a direct comparison of an internal surrogate (1D navigator) with a concurrently acquired external surrogate was reported (Li *et al* 2016). Multi-slice 2D acquisition based on navigator approaches can substantially reduce image artefacts compared with some of the image-derived approaches (Paganelli *et al* 2018) and could describe intra-cycle variations more effectively (Von Siebenthal *et al* 2007). One limitation of the navi-gator methods, however, is that they would require sequence modification and may result in longer acquisi-tion time, which is instead overcome by image-based approaches exploiting slice acquisition modality without a navigator. Nevertheless, parallel imaging solutions based on the simultaneous acquisition of image data and navigator can speed up scanning time (Celicanin *et al* 2015). Among the solutions reported in the literature (table 1), the sagittal orientation has been the most wide spread imaging direction, allowing reduced sorting artefacts

Table 1. Prospective and retrospective 4D MRI sorting methods based on multi-slice 2D image acquisitions.

	Method	Sorting	MR sequence	Slice orientation	Slice acquisition modality	Slice acquisition time [ms]
Von Siebenthal *et al* (2007)	2D navigator	Retrospective	2D bSSFP	Sagittal	Interleaved	≈180–190
Tokuda *et al* (2008)	1D navigator	Prospective	2D multi-slice GE/SE	Sagittal	Adaptive (interleaved)	n.a.
Cai *et al* (2011)	Body area	Retrospective	2D bSSFP	Axial	Cine	≈330
Wachinger *et al* (2012)	2D navigator + manifold learning	Retrospective	2D bSSFP	Sagittal	Interleaved	≈180–190
Tryggestad *et al* 2013b	External + average 4D MRI	Retrospective	2D bSSFP/SSFSE	Sagittal/ coronal	Interleaved/ ascending	≈300/400
Hu *et al* (2013)	External	Prospective	2D TSE	Axial/sagittal	Interleaved	≈270
Liu *et al* (2014)	Body area	Retrospective	2D bSSFP	Sagittal	Cine	≈500/600
Paganelli *et al* (2015c)	Image similarity	Retrospective	2D bSSFP	Sagittal	Interleaved	≈180
Du *et al* (2015)	External signal	Prospective	2D TSE	Sagittal	Interleaved	≈380
Liu *et al* (2015)	External signal + improved binning	Retrospective	2D SSFSE	Axial	Sequential	≈500
Fontana *et al* (2016)	Image similarity	Retrospective	2D bSSFP	Axial	Interleaved	≈400
Hui *et al* (2016)	Body area + Fourier-transform	Retrospective	2D bSSFP	Sagittal	Sequential (with manual slice adjustment)	≈160
Liang *et al* (2016)	External (probability-based)	Retrospective	2D bSSFP	Axial	Cine/sequential	n.a.
Uh *et al* (2016)	Dimensionality reduction	Retrospective	2D bSSFP	Sagittal	Alternating paired slices	≈330
To *et al* (2016)	External + visual feedback	Prospective	2D TSE	Coronal	Interleaved	≈400
Li *et al* (2017)	External/1D navigator	Prospective	2D TSE	Sagittal/ coronal	Sequential	≈500/700
Liu *et al* (2017)	Sagittal/coronal diaphragm point-of-intersection	Retrospective	2D bSSFP	Sagittal + coronal	Cine	330
van de Lindt *et al* (2018b)	Image simlarity	Retrospective	2D TSE	Axial	Interleaved	330
van de Lindt *et al* (2018a)	Image similarity	Retrospective	2D TSE/TFE	Coronal	Interleaved	316/366

bSSFP: balanced steady state free precession sequence (GE); SSFSE: single-shot fast spin echo; TSE: turbo-spin echo; TFE: turbo-field echo. n.a.: not available.

and a more comprehensive respiratory motion quantification (Liu *et al* 2014). However, the trade-off between acquisition time, field of view and resolution as well as the clinical experience derived from 4D CT, make axial acquisition an alternative anatomical direction to investigate (van de Lindt *et al* 2018b).

Alternative approaches that work directly in *k*-space rather than image-domain have also been investigated. These methods sort the *k*-space data into respiratory bins prior to reconstructing into image space (Buerger *et al* 2012, Feng *et al* 2014, 2016, Deng *et al* 2016, Rank *et al* 2016, Jiang *et al* 2017b, Küstner *et al* 2017, Mickevicius and Paulson 2017a, Weick *et al* 2017, Weiss *et al* 2017, Zucker *et al* 2017, Breuer *et al* 2018). In order to sort the data, a breathing signal can be extracted directly from the *k*-space, an approach which is referred to as self-gated or self-navigated acquisition. This is achieved by frequently sampling the centre of k-space, and using this data to form a 1D breathing signal. Many of the k-space based methods use radial acquisition schemes (Buerger *et al* 2012, Feng *et al* 2014, 2016, Deng *et al* 2016, Jiang *et al* 2017b, Mickevicius and Paulson 2017a, Zucker *et al* 2017) as these sample the centre of k-space with every spoke, making them well suited for self-gating, but cartesian acquisition schemes have also been used (Küstner *et al* 2017, Weick *et al* 2017, Breuer *et al* 2018).

Parallel imaging and under-sampling schemes (Heidemann *et al* 2003, Pruessmann 2006, Lustig *et al* 2008, McRobbie *et al* 2017), can be utilised to help maximize spatial coverage, to improve spatial resolution while respecting a clinically feasible total acquisition time of a few minutes or less (Feng *et al* 2014, Küstner *et al* 2017, Mickevicius and Paulson 2017a). Advanced approaches that use deformable image registration to include motion correction in the reconstruction process have been proposed for reducing the acquisition time even

further (37–41 s) while maintaining high quality images (Rank *et al* 2016, 2017), but this comes at the expense of long reconstruction times. A recent comparison of several methods showed that it is possible to get good quality images with a combined acquisition and reconstruction time of less than 5 min (Mickevicius and Paulson 2017a). Such methods hold promise for both planning and adapting radiotherapy treatments, but currently they are still 'research methods'. In fact, these require customised sequences and reconstruction methods and are not widely available on clinical scanners, limiting their use compared to some of the image-domain based methods.

3. MRI for organ motion management in treatment planning

In order to accurately design treatment plans in the presence of respiratory motion, accurate description of organ motion is required. In recent years, there has been substantial and growing efforts to incorporate time-resolved 2D and 4D MRI into radiotherapy treatment planning for organ motion management, either to complement CT or as the sole imaging modality (Schmidt and Payne 2015, Kashani and Olsen 2018).

3.1. MRI-guided treatment planning

3.1.1. Gated treatment approaches

In gated treatments, the treatment plan is designed assuming that the beam is only turned on when the tumour is in a pre-defined position, with a typical recommendation for gating windows that residual tumour motion is less than 5 mm (Keall *et al* 2006). In order to perform gating, a real-time indicator of tumour position is required and be consistent between planning and treatment. In conventional x-ray imaging, surrogates are typically acquired from implanted or external fiducials, with limitations due to invasiveness as well as poor correlation with internal anatomy (Ruan *et al* 2008, Park *et al* 2018). With this respect, MRI enables a non-invasive and more effective method to directly visualise target structures. Cine-MRI has been used to show that surrogacy uncertainties can cause gating errors of up to 38% (Liu *et al* 2004, Feng *et al* 2009, Cai *et al* 2010). Moreover, cine-MRI acquired at different sessions (2 week interval) was exploited for the definition of optimal gating windows (Liu *et al* 2004), based on the relationship between the lung and skin movement and accounting for inter- and intra- fraction breathing variability. Finally, the use of time-resolved MRI to directly derive an internal surrogate for gating purposes was proposed, and its application on the new in-room MRI integrated systems described (Crijns *et al* 2011, Mutic and Dempsey 2014) (section 4.1). For the planning of gated treatments with cine-MRI, the Viewray system relies on the acquisition of pre-treatment breath-hold MRI acquisitions (Acharya *et al* 2016, Bohoudi *et al* 2017). These are used for contour propagation from CT, considering safety margins to account for free-breathing variations during treatment (see section 4.2 for additional details).

Although gating approaches are used in radiotherapy, it has to be noted that planning and treating for only one phase of the breathing cycle allows one to 'freeze' tumour motion at the expense of reduced treatment efficiency and increased complexity.

3.1.2. ITV approaches

The most widely adopted approach to deal with anatomic motion in radiotherapy is to place a treatment margin around the target volume during the treatment planning phase (Van Herk 2004). In the case of respiratory motion, the treatment volume is typically expanded to encompass the full extent of tumour motion measured during planning. Treatment is then carried out, based on the assumption that the breathing cycle determined during planning is consistent and reproducible throughout treatment. This is the so-called 'internal target volume' (ITV) approach (ICRU 1999). Current standard of practice is to design the ITV based on 4D CT, which sorts data to derive a patient representative breathing cycle. Since substantial cycle-to-cycle breathing variations may occur, the ITV calculated on this single cycle may differ from the ITV obtained averaging over many breaths, with potential detriment of treatment accuracy (Ge *et al* 2013, Thomas *et al* 2017). In this context, the use of extended cine-MRI acquisitions has been demonstrated to detect larger differences in tumour motion (up to 1 cm) when compared with 4D CT, and therefore to reduce uncertainties associated with cycle-to-cycle breathing variations in the ITV, with improved margins definition (Cai *et al* 2008, Tryggestad *et al* 2013b, Akino *et al* 2014, Fernandes *et al* 2015, Park *et al* 2018). Cine-MRI was also used to generate maximum intensity projection images, which could be used to define the ITV (Adamson *et al* 2010). Based on these studies, the inclusion of dynamic MRI over extended imaging periods has the potential to increase the accuracy of motion encompassing treatment approaches, by providing a more comprehensive evaluation of motion at the planning phase. However, even assuming that motion encompassing planning techniques, such as ITV, can adequately compensate for tumour motion during treatment, they still suffer from the shortcoming that an increased amount of healthy tissue is irradiated (Ehrbar *et al* 2017).

3.1.3. Mid-position and probabilistic approaches

In the mid-position approach, the average position (or the phase closest to the average position in case of mid-ventilation) of the tumour throughout the breathing cycle is determined, and a planning volume defined around this (Wolthaus *et al* 2006, 2008). Such an approach results in smaller target volumes, but similar dosimetric outcomes compared to the ITV approach (Lens *et al* 2015). An extension to the mid-position approach is probabilistic treatment planning, in which treatment uncertainties are explicitly taken into account during the plan optimisation process (Li and Xing 2000, Unkelbach and Oelfke 2004).

As with ITV approaches, the major limitation of mid-position and probabilistic approaches is the limited amount of information on tumour motion provided by a single 4D CT scan, because the average position of the tumour may differ across different breathing cycles. It was demonstrated that cine-MRI imaging is useful for assessing the probability density function or mean tumour position on multiple breathing cycles, and that errors tend to decrease with extended imaging times, typically stabilizing after approximately three to five minutes (Cai *et al* 2006, 2008, Tryggestad *et al* 2013a). These results demonstrate the utility of dynamic MRI to enable more accurate treatment planning in mid-position and probabilistic approaches.

Acquiring mid-position images with MRI can be challenging due to the high velocity of the tumour at mid ventilation. One approach is to warp a high quality end-exhale image to the mid-ventilation using deformable image registration (van de Lindt *et al* 2016). Alternatively, (Stemkens *et al* 2017) proposed an approach in which a mid-position image is derived from a 4D MRI acquisition in a similar fashion as for 4D CT (figure 3). (McClelland *et al* 2017) presented a framework for fitting a motion model directly to unsorted multi-slice 2D data, so that they can be combined to form a high-quality 3D volume representing the time-averaged anatomy.

3.1.4. 4D planning

Treatment planning is typically carried out on a static anatomical image, even though it is known that the anatomy features a dynamic behaviour. An alternative approach is 4D planning, in which anatomical motion is explicitly taken into account during dose calculation and optimization, by calculating the plan on each phase of a 4D image and accumulating the dose or directly including the time dependence of the delivery fluence together with anatomical changes (Hugo and Rosu 2012, Rosu and Hugo 2012, Chang *et al* 2017).

For the case where a treatment plan is explicitly designed to be robust against motion (e.g. ITV or mid-posi-tion/ventilation), the differences between 3D and 4D dose calculations are usually minimal (Rosu and Hugo 2012). However, for advanced delivery strategies, such as multi-leaf-collimator tracking and active scanning proto n therapy (Chang *et al* 2017), the role of 4D planning may become more important. In these cases, 4D plan-ning can be used to generate a motion-robust plan, providing a better estimate of the delivered dose (Zhang *et al* 2014, Bernatowicz *et al* 2017, Al-Ward *et* al 2018).

The utility of 4D MRI in providing an extended 4D dataset for dose calculations was demonstrated in proton therapy, where organ motion can strongly affect the dose distribution (Boye *et al* 2013, Bernatowicz *et al* 2016, Zhang *et al* 2016). The method is based on using image registration to warp a static CT with the motion information provided from a 4D MRI, thus creating a combined 4D CT(MRI) dataset, which allows the cycle-by-cycle description of breathing motion. This approach allows the inclusion of respiratory organ motion into 4D dose calculations on the basis of the motion derived by the 4D MRI. A first validation of 4D dose calculation based on 4D CT(MRI) was recently provided by Bernatowicz *et al* (2016, 2017) for clinical liver cancer cases, in which 93% of dose calculation points were within 3%/3 mm for 4D dose calculations based on 4D CT and 4D CT(MRI) (figure 3). This approach is particularly useful to reduce the maximum dose to critical structures while maintaining target dose coverage in the presence of organ motion. However, a high sensitivity to motion vari-ability between the optimised and tested scenario was also described, as well as the restriction of the model to the target organ (e.g. lung and liver), which may result in a sub-optimal definition of the motion extracted at the structures next to the target.

3.2. MRI-based dose calculation

The most substantial limitation to the use of MRI in treatment planning is that MRI does not provide the electron density information needed for dose calculations. As such, research efforts were aimed at trying to approximate electron density directly from MR images (so-called 'pseudo-CT' or 'synthetic-CT'). Typically, dose calculation accuracy of within 2% with respect to the gold standard CT-based planning has been considered acceptable (Venselaar *et al* 2001, Edmund and Nyholm 2017). Various techniques exist to approximate electron density data from MRI, such as bulk-density, atlas-based or machine learning solutions (Edmund and Nyholm 2017). These were investigated in great detail for 3D MRI imaging, particularly in relatively homogenous sites such as the brain and pelvis, and MRI-based planning was successfully integrated in clinical workflows (Edmund and Nyholm 2017, Johnstone *et al* 2017), with some early work also carried out for proton therapy (Maspero *et al* 2017). On the other hand, synthetic-CT generation in sites affected by respiratory motion (e.g. lung, liver, breast, pancreas and kidney) has been far less investigated, with only one published paper that investigated MRI-based planning

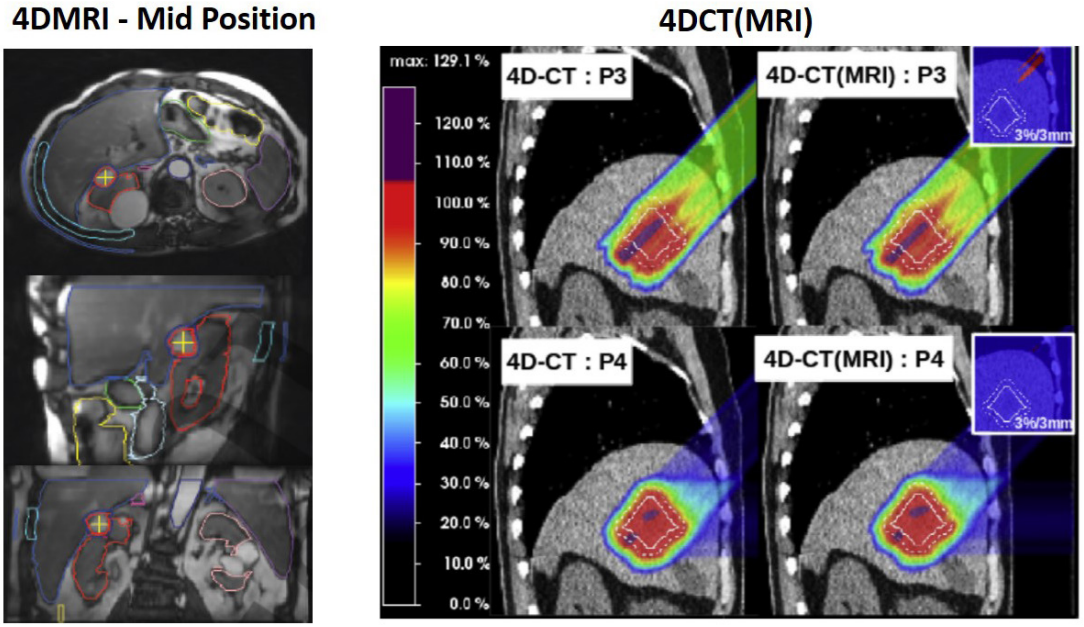

Figure 3. 4D MRI in treatment planning. 4D MRI acquisitions with contours defined on the mid-position on the left (reprinted with permission from Stemkens *et al* (2017)). 4D CT versus 4D CT (MRI) approaches for proton dose calculation on the right (reprinted with permission from Bernatowicz *et al* (2016)).

in sites affected by motion (Jonsson *et al* 2010). The reasons for this are twofold. First, these sites tend to have more complex and heterogeneous electron density distributions, caused by a wider variety of tissue types (e.g. lung, bone and soft tissue). This means that errors in the synthetic-CT data are more likely to produce errors in dosimetry compared to homogeneous sites such as brain. Second, the presence of substantial respiratory motion makes the accurate generation of electron density data particularly challenging.

For ITV, mid-position/ventilation, or respiratory gating, 3D electron densities may be sufficient for planning, if 4D dose optimisation or tumour tracking is applied, electron density is desired for the full 4D dataset. A first order approach to derive a pseudo-CT, consists in the previously mentioned bulk-density assignment (Kerkhof *et al* 2010), in which an automatically generated body contour is filled with Hounsfield Units equal to water, while other voxels are set to air. This approach has been investigated in abdominal sites for both static (Stam *et al* 2013a) and motion-compensated planning relying on 4D MRI data (Glitzner *et al* 2015a, Stemkens *et al* 2017). Another solution is the previously mentioned 4D CT(MRI) approach, which uses the motion information provided by 4D MRI to warp a 3DCT dataset relative to one single respiratory phase (Boye *et al* 2013).

4. MRI for organ motion management in treatment delivery

Besides the integration of MRI into radiotherapy treatment planning (section 3), a substantial impact is expected from the use of MRI image guidance during treatment delivery, which is now available through a new generation of combined in-room MRI-treatment units. The use of such systems is expected to allow on-line image acquisitions just before and during treatment. This aims at quantifying inter- and intra-fraction anatomo-pathological changes by means of imaging, which could be used to accurately deliver the planned dose based on the current changing anatomy or to entirely create a new plan, thus performing adaptive treatments (Verellen *et al* 2008, Hunt *et al* 2018).

4.1. In-room MRI radiotherapy systems

A number of in-room MRI-guidance systems are described in the literature (Fallone 2014, Jaffray *et al* 2014, Keall *et al* 2014, Lagendijk *et al* 2014, Mutic and Dempsey 2014), two of which developed by commercial entities and treating patients: the Viewray MRIdian system and the Elekta-Unity system (figure 4, panel (A)). The first treatments were carried out using the Cobalt-based Viewray MRIdian in 2014 (Olsen *et al* 2014), while the world's first MRI-Linac treatment using the Elekta-Unity was in 2017 (Raaymakers *et al* 2017). Both systems utilize configurations in which the treatment beam is oriented perpendicular to the magnetic field (figure 4, panel (B)). In this configuration, the superior/inferior axis of patient is aligned with the magnetic field in the same manner as a conventional MRI scanner, and the linac can rotate independently of the magnet and patient. However, magnetic fields applied perpendicular to the treatment beam can substantially perturb dose deposition compared to zero field situation, particularly for the higher field Elekta-Unity system. In many situations, these

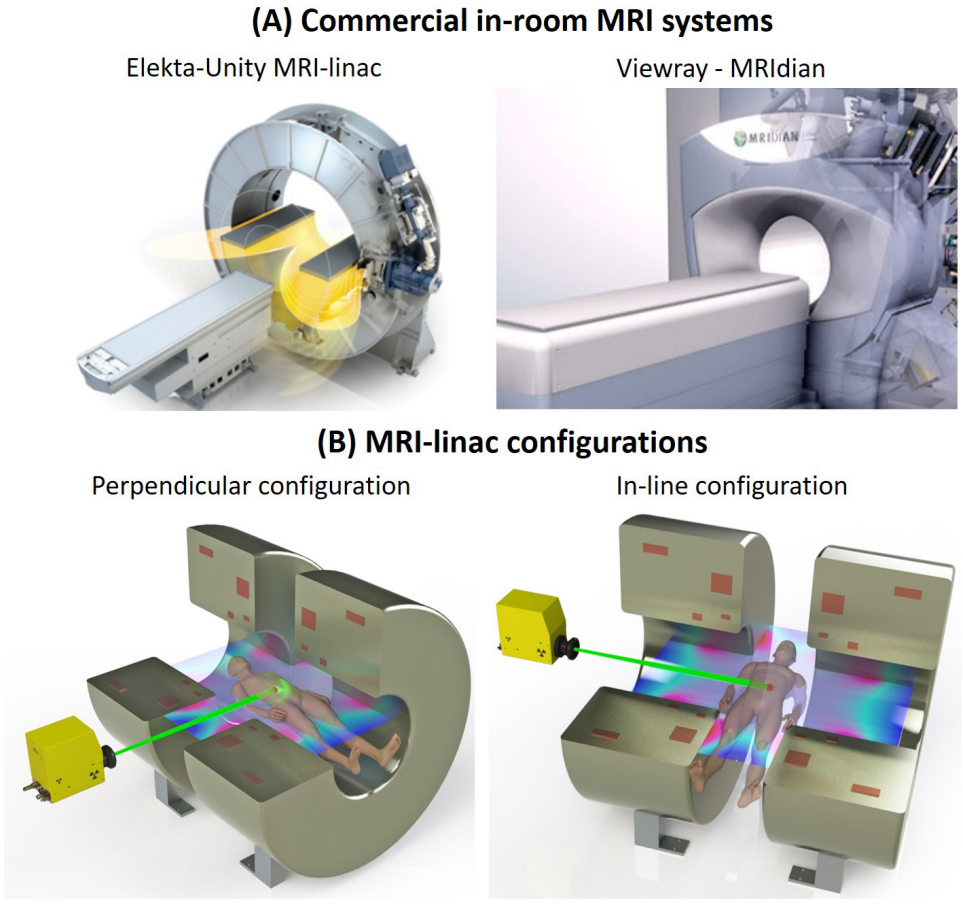

Figure 4. In-room MRI systems. (A) Commercial systems: Elekta-Unity MRI-linac and viewray MRIdian. (B) MRI-linac configurations: MRI-linac systems can be constructed in either the perpendicular configuration, or the in-line configuration (the images shown here are based on the Australian prototype system, which was designed to facilitate operation in both configurations).

effects can be compensated for using advanced treatment plan optimisation strategies (Raaijmakers *et al* 2007). An alternative approach is to change the relative configuration of the radiation source and MRI scanner, such that the treatment beam and the magnetic field of the MRI scanner are parallel to each other (the 'in-line' approach, figure 4, panel (B)). This approach is being developed independently by two academic groups, and can minimize or even exploit the effect of the magnetic field on the dose distribution via penumbral trimming and electron focusing effects (Oborn *et al* 2016, Alnaghy *et al* 2017). However, the same physical mechanisms can also cause problems in certain scenarios, with increases in skin dose up to 1400% observed (Oborn *et al* 2014). It appears that this problem can be largely mitigated either through optimisation of the magnetic fringe field or electron purging devices (Keyvanloo *et al* 2012, Oborn *et al* 2014). From a device perspective, the disadvantage of the in-line approach is that substantial redesign of the MRI magnet is required, and that in order to provide rotation between the beam and the patient, either the MRI scanner or the patient must be rotated, both of which are challenging (Keall *et al* 2014, Whelan *et al* 2017).

A solution which avoids all of these problems is the MRI-on-rails approach (Jaffray *et al* 2014), in which a 'near-room' MRI scanner can be moved into the treatment room for pre-treatment imaging, and removed afterwards. This approach has the advantage that the magnet can be used for multiple purposes, little redesign of existing equipment is required, and interference between the MRI scanner and radiotherapy equipment is minimized. On the other hand, the MRI cannot be used for intra-fraction monitoring, and additional time is required to move the MRI scanner in and out of the room. A similar approach using a 1.5 T scanner was developed in Umea in which the patient rather than the MRI scanner is moved (Karlsson *et al* 2009, Menten *et al* 2017), although this system has recently been decommissioned and replaced with a PET/MRI scanner (Brynolfsson *et al* 2018). Table 2 shows a comparison of existing in-room/near-room MRI systems.

In addition to the existing in-room MRI systems for photon-based treatments, recent studies have started investigating the possibility of integrating MRI with particle therapy (Hartman *et al* 2015, Kurz *et al* 2017, Oborn *et al* 2017). This concept combines the high precision of particle therapy with the high accuracy enabled by in-room MRI. However, the engineering challenges inherent to in-room photon guided system are magnified for particle systems, due to the size and complexity of these particle therapy gantries, and the use of large scanning

Table 2. Comparison of existing in-room or near-room MRI systems.

System	X-ray source	Status	Field orientation	Field strength	Gradient strength/slew rate
Elekta-Unity	7 MV linac	Commercial system	Perpendicular	1.5 T	15 mT m^{-1} 65 T/m/s
Viewray MRIdian	Cobalt or 6 MV linac	Commercial system	Perpendicular	0.35 T	18 mT m^{-1} 200 T/m/s
Australia	6 MV linac	Research prototype	In-line/ perpendicular	1.0 T	10 mT m^{-1} 225 T/m/s
Alberta/MagnetTx	6 MV linac	Research prototype	In-line	0.56 T	20 mT m^{-1} 66 T/m/s
Princess margaret hospital	Varian TrueBeam linac	One off clinical facility	n.a.	1.5 T	33 mT m^{-1} 170 T/m/s
Umea University (near-room)	Siemens Oncor linac	One off clinical facility	n.a.	1.5 T	33 mT m^{-1} 170 T/m/s

n.a.: not applicable.

magnets which must be rapidly switched to steer the beam. In addition, magnetic fields distort particle beams and this must be compensated for. These issues were investigated in a recent publication by Oborn *et al* (2017).

4.2. MRI-guided treatment delivery

4.2.1. Inter-fraction motion management

Inter-fraction motion management refers to the acquisition of imaging data before each treatment session to daily quantify anatomo-pathological changes for an accurate delivery of the planned dose.

In MRI-guided treatments, there have been promising results on the use of MRI for on-line inter-fraction motion quantification of pancreatic (Jiang *et al* 2017a) and breast cancers (Acharya *et al* 2016) using the Viewray system. In a recent application of MRI in gated treatments (Bohoudi *et al* 2017), high-resolution volumetric MR images of the patient were acquired immediately prior to treatment, and deformable image registration with automatic contour propagation used to account for inter-fractional changes and subsequent plan delivery. In the first experience for pancreatic stereotactic body radiotherapy, contours were first propagated from the planning scan and then manually re-contoured within 3 cm from the PTV (Planning Target Volume), while the patient was in treatment position. For ITV treatment approaches, in-room MRI was used to demonstrate that the extent of motion can differ substantially among different treatment fractions, resulting in differences in the ITV of up to 46% (Thomas *et al* 2017). The latter study highlights the potential of in-room time-resolved MRI, which allowed the authors to capture extended image data for over 20 min. For mid-position approaches, recent studies described the acquisition of a 4D MRI to derive on-board mid-position images with in-room MRI (Kontaxis *et al* 2017, Stemkens *et al* 2017).

A potential issue using current MRI-Linacs systems is that couch motion is very limited. In conventional workflows, the couch is moved to facilitate the alignment of patient and beam coordinate systems (Caillet *et al* 2017). Due to the constrained geometry of MRI-Linac systems (figure 4), non-axial couch motion is either limited or non-existent. However, it has been demonstrated that couch shifts can be replaced by a 'virtual couch shift' technique, which utilises the multi-leaf-collimator to shift the plan to the new target position (Bol *et al* 2013, Ruschin *et al* 2017). Alternatively, the creation of a new plan directly before treatment was investigated in the Viewray (Acharya *et al* 2016, Bohoudi *et al* 2017) and Elekta-Unity systems (Raaymakers *et al* 2017) (see sec-tion 4.3 for details), without the necessity of couch shifts.

4.2.2. Intra-fraction motion management

A number of approaches exist both in photon and particle therapy to account for intra-fraction motion (Kubiak 2016, Caillet *et al* 2017), however they typically rely on the correlation between internal markers and external surrogates, rather than directly monitoring the tumour. Time-resolved MRI overcome this limitation and as such is an ideal modality for intra-fraction motion monitoring. By exploiting combined MRI-Linac systems, time-resolved MRI will become a core intra-fraction tool for MRI-guided treatments, providing real-time anatomy monitoring and facilitating multi-leaf-collimator adaptation for an accurate delivery of the planned dose.

MRI-based intra-fraction monitoring is strongly subject to considerations of spatial and temporal trade-offs (section 2). As such, fast 2D cine-MRI has been the most investigated technique (Koch *et al* 2004, Plathow *et al* 2004, Heerkens *et al* 2014, Paganelli *et al* 2015b), with the acquisition of interleaved orthogonal (sagittal/coronal) cine-MRI slices intersecting the target to track the 3D position of the tumour (Bjerre *et al* 2013, Tryggestad *et al* 2013a, Brix *et al* 2014, Sawant *et al* 2014, Paganelli *et al* 2015a, Stemkens *et al* 2016).

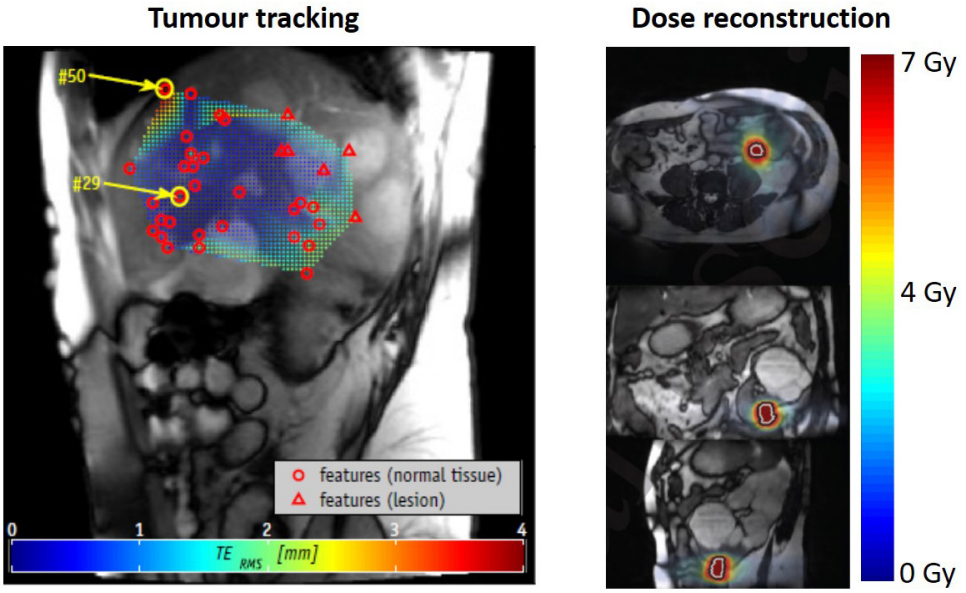

Figure 5. Time-resolved MRI in treatment delivery. An example of tumour tracking approach by means of anatomical landmarks on the left (reprinted with permission from Paganelli *et al* (2015b)). Dose reconstruction by means of a global motion model on the right (reprinted with permission from Stemkens *et al* (2017)).

In addition, intra-fraction use needs real-time automatic image processing methods to extract motion information from the high-frequency cine-MRI data. Several methods were investigated such as template matching, neural networks, particle filters, landmark extraction strategies (figure 5) and image registration (relevant references in table 3). Fast *et al* (2017) compared some of these methodologies in lung and showed that image-based 2D tumour motion estimation is feasible with all the investigated algorithms. However, based on their results, template matching provides the best compromise between flexibility, speed and accuracy. In a study con-ducted by Glitzner *et al* (2015b), the delay attributed to the multi-leaf collimator adaptation was shown to be a minor contributor to the overall feedback chain as compared to the impact of imaging components such as MRI acquisition and processing (Borman *et al* 2018), which therefore require mitigation strategies to predict tumour motion (Krauss *et al* 2011, Yun *et al* 2012, Seregni *et al* 2016).

The main issue with the use of 2D cine-MRI for intra-fraction monitoring is that it is difficult to track motion in the out-of-plane direction, which can result in anatomical structures appearing and disappearing from view accordingly. A possible solution is to derive the full 3D anatomical information based on one or two dimensional data, by using global motion modelling (McClelland *et al* 2013). To build such a model, first the motion is measured off-line from 4D pre-treatment images. The model is then fitted relating the motion to the surrogate data. Finally, during treatment the model is used to estimate the full 3D motion from the measured surrogate data. Global motion models have been extensively investigated for a wide range of applications and imaging modalities (McClelland *et al* 2013), including the use of MRI data to provide the motion measurements and/or the surrogate data when planning and guiding radiotherapy (Fayad *et al* 2012, Harris *et al* 2016, Stemkens *et al* 2016, 2017, McClelland *et al* 2017).

However, motion models have not yet entered widespread clinical use, due to two main problems. Firstly, the relationship between the motion and surrogate data can deteriorate over time due to changes in the breath-ing pattern and anatomy. Secondly, the images used to measure the motion are usually respiratory-correlated, and hence do not provide a good representation of the true motion including the intra-cycle variation, and its relationship to the surrogate data (Harris *et al* 2016, McClelland *et al* 2017). The use of in-room MRI systems may help alleviate the first problem, as the models can be built and updated just prior to, and even during treat-ment delivery. The second problem can be partly addressed by the use of 4D MRI methods that try to image the intra-cycle variation (Bernatowicz *et al* 2016). Alternatively, methods have been proposed that can fit the motion model directly to all the unsorted image data simultaneously (Odille *et al* 2008, McClelland *et al* 2017).

4.3. Dosimetric evaluation and adaptation

Many of the strategies outlined above are focused on geometric motion quantification by means of image acquisition to ensure target coverage and accurately deliver the planned dose. However, an adaptive treatment strategy should also adapt treatments in response to dose. Such a workflow is termed 'closed-loop' adaptive radiotherapy, in which the adaptive decision is made on the basis of optimal dose versus dose delivered and the

Table 3. Methods for tumour tracking based on cine-MRI acquisitions.

Method	Authors	Site	Field strength [T]	MR sequence	Slice orientation	Image acquisition time [ms]	Image resolution [mm]	Method accuracy [mm]	Processing time
Template matching	Koch *et al* (2004)	Lung	1.5	Fast GE	Sagittal/ coronal	450	n.p.	1–2	n.a.
	Cervino *et al* (2011)	Lung	3	n.a.	Sagittal	250	1.37 × 1.37 × 10	0.6	84 ms
	Tryggestad *et al* (2013a)	Lung	1.5	bSSFP	Sagittal/ coronal	250	2 × 2 × 5	0.7–1.6	n.a.
	Bjerre *et al* (2013)	Kidney	1.5	bSSFP	Sagittal/ coronal	252	1.05 × 1.05 × 7	1.15	153 ms
	Brix *et al* (2014)	Liver	1.5	bSSFP	Axial/ sagittal/ coronal	184	1.56 × 1.56 × 1.6	1.6	90 ms
	Shi *et al* (2014)	Lung	1.5	bSSFP	Sagittal	250	1.95 × 1.95 × (12–16)	1.95	10–15 s
	Fast *et al* (2017)	Lung	1.5	bSSFP, spoiled GE	Sagittal/ coronal	500	1.5 × 1.5 × 3.0	1.7	1 ms
Neural networks, particle filters	Cervino *et al* (2011)	Lung	3	n.p.	Sagittal	250	1.37 × 1.37 × 10	1.5	150 ms
	Gou *et al* (2014)	Liver, Pancreas, stomach	1.5	bSSFP	Coronal	200	1.87 × 1.87 × 7	0.70–0.92 (DSC)	1.8–33 s
	Yun *et al* (2015)	Lung	0.5	bSSFP	Sagittal	280	3.1 × 3.1 × 20	0.5–0.9	40 ms
	Lee *et al* (2016)	Lung	1.5	bSSFP	Sagittal/ coronal	303	1.48 × 1.48 × 5	n.a.	n.a.
	Bourque *et al* (2016)	Lung	1.5	bSSFP	Sagittal	250	1.0 × 1.0 × 10.0	0.6–2	0.8–2
	Fast *et al* (2017)	Lung	1.5	bSSFP, spoiled GE	Sagittal/ coronal	500	1.5 × 1.5 × 3	2	25 ms
Internal landmarks	Paganelli *et al* (2015b)	Liver	1.5	bSSFP	Sagittal (oblique)	310	1.28 × 1.28 × 10	1.87	≈15 min
	Paganelli *et al* (2015a)	Lung	1.5	bSSFP	Sagittal/ coronal	303	1.48 × 1.48 × 5	1.87	≈15 min
	Mazur *et al* (2016)	Lung	0.35	bSSFP	Sagittal	250	3.5 × 3.5 × 7	1.4	≈250 ms
	Fast *et al* (2017)	Lung	1.5	bSSFP, spoiled GE	Sagittal/ coronal	500	1.5 × 1.5 × 3	2	150 ms
Image Registration	Sawant *et al* (2014)	Lung	1.5	bSSFP	Sagittal/ coronal	152-273	2 × 3 × 5	n.a.	n.a.
	Heerkens *et al* (2014)	Pancreas	1.5	SSFP	Sagittal/ coronal	500	1.4 × 1.4 × 5	n.a.	n.a.
	Zachiu *et al* (2015)	Kidney, liver	1.5	Single-shot GE	Coronal	83	2.5 × 2.5 × 7	≈2.5	≈25 ms
	Seregni *et al* (2017)	Liver	1.5	bSSFP	Sagittal (oblique)	310	1.28 × 1.28 × 10	1.28	50 ms
	Fast *et al* (2017)	Lung	1.5	bSSFP, spoiled GE	Sagittal/ coronal	500	1.5 × 1.5 × 3	1.7	500 ms

n.a.: not available.
bSSFP = balanced steady state free procession; SPGR = spoiled gradient echo; EPI = echo planar imaging.

plan re-optimised (de la Zerda *et al* 2007). As for the geometrical scenario, dose adaptation can be carried out both inter- and intra-fractionally.

Whilst the potential of inter-fraction adaptation has been deeply discussed in the literature, it is only with the advent of in-room MRI-guidance that this became a vendor supported on-line clinical reality. Inter-fraction dose adaptation is in fact implemented on the Viewray system (Acharya *et al* 2016, Bohoudi *et al* 2017), where deformable registration is used to propagate contours and Hounsfield units from the planning data, and dose calculation is performed and compared to the planned dose. A manual review triggers a decision on whether plan re-optimisation should be performed. A recent prospective trial reported promising results of this adaptive

protocol in PTV dose escalation and/or simultaneous organs at risk sparing for the treatment of oligometastatic or unresectable primary malignancies of the abdomen (Henke *et al* 2018). An alternative workflow was demonstrated in a trial setting using the Elekta-Unity system (Raaymakers *et al* 2017), in which plan re-optimisation was carried out automatically. Both workflows utilise fast Monte-Carlo based dose engines to minimise the time for re-planning. For the Viewray system, new plans can be generated in approximately 12 min, including manual review and re-contouring (Bohoudi *et al* 2017). Plan generation using the Elekta-Unity system was reported to take approximately 5 min in a clinical setting (Raaymakers *et al* 2017), whilst in the research setting, plan generation ranged from seconds to minutes (Bol *et al* 2012). In addition, pre-beam re-planning supported by fully automatic contours propagation could save time (Kontaxis *et al* 2017).

On the other hand, intra-fraction dose adaptation has yet to be clinically demonstrated but remains a tantalising prospect. An intriguing approach to this problem was recently proposed by Kontaxis *et al* (2015b), in which authors updated the treatment plan in response to the changing patient anatomy. This algorithm fundamentally differs from conventional approaches, which seek an 'optimal' solution before treatment is started. Instead, if the first delivered beamlet is sub-optimal, this is corrected via modulation of later applied beamlets, with the algorithm converging towards the ideal dose at the same time as the dose is being delivered. This approach can compensate for both inter and intra-fraction variation, as was clearly described and demonstrated by Kontaxis *et al* (2015a). However, uncertainties in deformable image registration algorithms, as well as the computational time required by the algorithm, still represent a limitation to clinical application.

As previously discussed (section 3.2), a major challenge for inter- and intra-fraction MRI-based dosimetric adaptation is that MRI images do not provide the electron density data needed for dose calculation. To date, the most commonly proposed approach to derive in-room electron density maps for moving targets is to propagate existing electron density information to daily MR images by using deformable image registration (Bohoudi *et al* 2017, Raaymakers *et al* 2017) or bulk-density overrides (Glitzner *et al* 2015a, Stemkens *et al* 2017). Alternatives include using a 4D CT(MRI) approach (Boye *et al* 2013, Marx *et al* 2014) or global motion models (Stemkens *et al* 2017) (figure 5). Although neither of these methods are currently implemented in real-time, they could be applied retrospectively to enable intra-fraction dose reconstruction and accumulation (Bernatowicz *et al* 2016, Stemkens *et al* 2017).

5. Conclusions and future directions

5.1. Roadmap for MRI-guidance in moving organs

MRI offers exquisite soft tissue contrast, unparalleled acquisition flexibility, dose-free imaging and functional acquisition. Due to these advantages, there is rapidly growing interest in the role of MRI in radiotherapy and in its use for organ motion management. This has motivated institutional, commercial and research efforts towards the implementation of advanced strategies to accomplish motion management. Based on the reported findings, we provide here a roadmap for an optimal use of MRI-guidance in radiotherapy, covering both treatment planning and delivery. This aims at supporting further research and potential clinical applications in the near-term. Specifically, from the literature analysis we can derive that:

- In treatment planning, both time-resolved 2D images and 4D MRI should be exploited to account for inter- and intra-fraction breathing variabilities. This will allow improved definition of personalized margin recipes and could be included in gating as well as ITV or mid-position approaches. Respiratory-correlated 4D MRI can further provide a dataset for robust planning and complement 4D CT. As reported in Chang *et al* (2017), 4D imaging should be exploited to enable 4D optimization which can improve plan robustness to intra-fractional motion for particle treatments or multi-leaf collimator tracking strategies. Vendors are therefore encouraged to implement motion analysis tools, dynamic dose calculation and 4D robust optimization within treatment planning systems. Due to the lack of MRI-based dose planning and calculation strategies in moving organs, the 4D CT(MRI) approach represents an attractive strategy to preserve electron density information. In this case, respiratory phase correspondence and/or image registration algorithms between CT and MRI need to be validated, to provide an accurate motion description. MRI (and/or 4D MRI) can be also exploited to perform multiple/frequent acquisitions to determine whether adaptive re-planning is needed to maintain plan robustness. This is especially the case for particle centres or institutions in which in-room MRI systems are not available.
- In treatment delivery with in-room MRI systems, pre-beam/on-board images are acquired before beam on, to update the plan or to create a new one. In this case, fast treatment planning and adaptation is performed as done by the MRIdian (Viewray) and Elekta-Unity treatment devices. On-line verification and quality assurance strategies for such adaptations are essential in the development of these approaches. An independent dose calculation engine could be used for verification, and retrospective dose reconstruction performed off-line.

During delivery, orthogonal sagittal/coronal cine-MR images should be acquired to allow the 3D motion estimation at the centre of the tumour. Alternatively, the sagittal direction is the favoured orientation in the literature to capture the major motion directions, and/or patient-specific evaluation based on treatment planning data could be investigated to determine the optimal cine-MRI orientation. In combination with cine-MRI acquisition, real-time tumour localization methods are likely to be implemented and integrated in the treatment workflow. These methods are essential for residual motion quantification in the gating window and for tumour tracking and multi-leaf collimator adaptation. Template matching has been shown in the literature to be an attractive solution since it is simple, robust and fast to test. However, in case of tumour tracking treatments, improvements of this approach should be considered to account for non-rigid displacements as well as effects of out-of-plane motion. These could be supported by pre-beam/on-board 4D MRI and retrospective evaluations such as motion models. Additionally, prediction algorithms need to be considered when system latencies hinder acquiring information in real-time. Another important aspect to take into consideration for in-room MRI systems is the request for on-line dose evaluation and adaptation, which should be supported by vendors and integrated in the treatment workflow. Bulk-density analysis could be performed as preliminary approach for on-line verification of planned dose versus delivered dose, since in online adaptive scenarios it may be acceptable to have a lower threshold for dose calculation accuracy than for planning. Off-line verification should also be performed in this case, for example by utilising global motion models for dose accumulation.

5.2. Future challenges

Despite the potential of MRI in radiotherapy, there are a number of challenges to increasing its clinical penetration. To overcome these, technological and methodological improvements are required.

The first issue for organ motion management with MRI is the inherent trade-off between spatial and temporal resolution. The ultimate goal of 'real-time' 4D imaging (approximately four or more 3D volumes per second with appropriate spatial resolution) remains some distance in the future. At present, state-of-the-art imaging for motion compensation relies on time-resolved 2D cine-MRI data, which can deliver approximately four inter-leaved images per second. As far as 4D imaging is concerned, several approaches have been proposed relying on retrospective sorting of images or k-space data as well as motion modelling. However, further research is needed to define standards for the clinical inclusion of 4D MRI in the radiotherapy workflow.

MRI does not provide the electron density information needed for treatment planning and/or dose delivery verification. This must be overcome for fully MRI-guided treatment. For static anatomical sites such as pelvis and brain, electron density recovery from MRI images has been investigated quite extensively within the literature, and commercial products have recently been released. However, for anatomical sites where substantial motion occurs, further research is required to ensure accurate MRI-based dose calculation. Moreover, it is also important to note that MRI suffers from geometrical distortion which could affect MRI-based dose calculation and organ motion quantification. This aspect was reviewed in Schmidt and Payne (2015) and, to our knowledge, just one publication has been reported dealing with moving organs (Torfeh *et al* 2018). Effects of geometrical distortion are outside the scope of this review but require additional evaluation on the accuracy of MRI for treatment guid-ance and protocols should be defined to account for these uncertainties.

An additional advantage of MRI with respect to x-ray imaging is the possibility to derive functional information, which has the potential to enable increased treatment personalisation across the entire radiotherapy work-flow (van der Heide *et al* 2012, Prestwich *et al* 2015, Bainbridge *et al* 2017a). However, most of functional MRI techniques in regions affected by motion under free-breathing are still in a very preliminary stage. Perfusion MRI and diffusion MRI have been investigated with in-room MRI systems to enhance tumour visibility (Wojcieszyn-ski *et al* 2016) or preliminary assess tumour response (Yang *et al* 2016), but few studies dealt with organ motion management (Liu *et al* 2016b). Functionally guided planning in the lung based on hyperpolarised MRI showed potentials in reducing the amount of healthy tissue irradiated and has been used to prospectively treat patients in the experimental arm of the double-blind randomised functional lung avoidance for individualized radiother-apy (FLAIR) trial (Hoover *et al* 2014). Additionally, the potential of PET/MRI has been demonstrated in both treatment planning (Brynolfsson *et al* 2018) and tumour response assessment (Varoquaux *et al* 2015, Daniel *et al* 2017), with attainable results in providing anatomical and functional 4D maps (Fayad *et al* 2017). However, fur-ther research is required in sites affected by organ motion and replication and standardization are needed before these techniques achieve the level of clinical confidence required in a treatment workflow.

In conclusion, guidelines and quality assurance strategies for clinical applications of MRI in organ motion management need to be defined to support the move of radiotherapy towards high precision techniques and personalised treatment. The growing experience in the use of MRI-Linacs is expected to contribute significantly towards this goal, especially with the support of clinical studies to evaluate the clinical impact of MRI-guided radiotherapy in sites affected by organ motion.

Acknowledgments

The authors would like to thank Dr Teo Stanescu (Princess Margaret Cancer Centre, Toronto, Canada), Dr Gino Fallone (University of Alberta, Edmonton, Canada) and Dr Tufve Nyholm (Umea University, Umea, Sweden) for providing information on the Princess Margaret, Alberta/MagnetTx in-room MRI systems and Umea system, respectively. MF and TvdL would like to acknowledge that The Netherlands Cancer Institute is part of the Elekta Atlantic MR-Linac research consortium. JMC and BE are funded by the Stand Up to Cancer campaign for Cancer Research UK (C33589/CRC521) and Network Accelerator Award Grant (A219932). In addition, we would also like to acknowledge the important contributions of the anonymous reviewers.

Conflict of interest

CP, BW, MP, PS, MF, TvdL, JMC, BE, TL, MR, GB have no conflict of interest.

PK is a stakeholder in SeeTreat, a start-up company to commercialize intellectual property generated through NHMRC program grant APP1036075 'The Australian MRI-Linac program'.

ORCID iDs

C Paganelli https://orcid.org/0000-0003-4787-8649
B Whelan https://orcid.org/0000-0002-2326-0927
P Summers https://orcid.org/0000-0002-5085-1095
M Fast https://orcid.org/0000-0001-9107-4627
J McClelland https://orcid.org/0000-0002-4922-0093
M Riboldi https://orcid.org/0000-0002-2431-4966

References

Acharya S, Fischer-Valuck B W, Kashani R, Parikh P, Yang D, Zhao T, Green O, Wooten O, Li H H and Hu Y 2016 Online magnetic resonance image guided adaptive radiation therapy: first clinical applications *Int. J. Radiat. Oncol. Biol. Phys.* **94** 394–403

Adamson J, Chang Z, Wang Z, Yin F F and Cai J 2010 Maximum intensity projection (MIP) imaging using slice-stacking MRI *Med. Phys.* **37** 5914–20

Akino Y, Oh R J, Masai N, Shiomi H and Inoue T 2014 Evaluation of potential internal target volume of liver tumors using cine-MRI *Med. Phys.* **41** 111704

Alnaghy S J, Begg J, Causer T, Alharthi T, Glaubes L, Dong B, George A, Holloway L and Metcalfe P 2017 Penumbral width trimming in solid lung dose profiles for 0.9 T and 1.5 T MRI-linac prototypes *Med. Phys.* **45** 479–87

Al-Ward S M, Kim A, McCann C, Ruschin M, Cheung P, Sahgal A and Keller B M 2018 The development of a 4D treatment planning methodology to simulate the tracking of central lung tumors in an MRI-linac *J. Appl. Clin. Med. Phys.* **19** 145–55

Bainbridge H E, Menten M J, Fast M F, Nill S, Oelfke U and McDonald F 2017b Treating locally advanced lung cancer with a 1.5 T MR-linac-effects of the magnetic field and irradiation geometry on conventionally fractionated and isotoxic dose-escalated radiotherapy *Radiother. Oncol.* **125** 280–5

Bainbridge H, Salem A, Tijssen R H, Dubec M, Wetscherek A, Van Es C, Belderbos J, Faivre-Finn C, McDonald F and lung tumour site group of the international Atlantic MR-Linac Consortium 2017a Magnetic resonance imaging in precision radiation therapy for lung cancer *Transl. Lung Cancer Res.* **6** 689–707

Barth M, Breuer F, Koopmans P J, Norris D G and Poser B A 2016 Simultaneous multislice (SMS) imaging techniques *Magn. Reson. Med.* **75** 63–81

Barton M B, Jacob S, Shafiq J, Wong K, Thompson S R, Hanna T P and Delaney G P 2014 Estimating the demand for radiotherapy from the evidence: a review of changes from 2003 to 2012 *Radiother. Oncol.* **112** 140–4

Bernatowicz K, Peroni M, Perrin R, Weber D C and Lomax A 2016 Four-dimensional dose reconstruction for scanned proton therapy using liver 4D CT-MRI *Int. J. Radiat. Oncol. Biol. Phys.* **95** 216–23

Bernatowicz K, Zhang Y, Perrin R, Weber D C and Lomax A J 2017 Advanced treatment planning using direct 4D optimisation for pencil-beam scanned particle therapy *Phys. Med. Biol.* **62** 6595

Biederer J, Hintze C, Fabel M and Dinkel J 2010 Magnetic resonance imaging and computed tomography of respiratory mechanics *J. Magn. Reson. Imaging* **32** 1388–97

Bjerre T, Crijns S, af Rosenschöld P M, Aznar M, Specht L, Larsen R and Keall P 2013 Three-dimensional MRI-linac intra-fraction guidance using multiple orthogonal cine-MRI planes *Phys. Med. Biol.* **58** 4943

Blackall J, Ahmad S, Miquel M, McClelland J, Landau D and Hawkes D 2006 MRI-based measurements of respiratory motion variability and assessment of imaging strategies for radiotherapy planning *Phys. Med. Biol.* **51** 4147

Bohoudi O, Bruynzeel A, Senan S, Cuijpers J, Slotman B, Lagerwaard F and Palacios M 2017 Fast and robust online adaptive planning in stereotactic MR-guided adaptive radiation therapy (SMART) for pancreatic cancer *Radiother. Oncol.* **125** 439–44

Bol G, Hissoiny S, Lagendijk J and Raaymakers B 2012 Fast online Monte Carlo-based IMRT planning for the MRI linear accelerator *Phys. Med. Biol.* **57** 1375

Bol G, Lagendijk J and Raaymakers B 2013 Virtual couch shift (VCS): accounting for patient translation and rotation by online IMRT re-optimization *Phys. Med. Biol.* **58** 2989

Borman P, Tijssen R, Bos C, Moonen C, Raaymakers B and Glitzner M 2018 Characterization of imaging latency for real-time MRI-guided radiotherapy *Phys. Med. Biol.* **63** 155023

Bourque A E, Bedwani S, Filion É and Carrier J F 2016 A particle filter based autocontouring algorithm for lung tumor tracking using dynamic magnetic resonance imaging *Med. Phys.* **43** 5161–9
Boye D, Lomax T and Knopf A 2013 Mapping motion from 4D-MRI to 3D-CT for use in 4D dose calculations: a technical feasibility study *Med. Phys.* **40** 061702
Breuer K, Meyer C B, Breuer F A, Richter A, Exner F, Weng A M, Ströhle S, Polat B, Jakob P M and Sauer O A 2018 Stable and efficient retrospective 4D-MRI using non-uniformly distributed quasi-random numbers *Phys. Med. Biol.* **63** 075002
Brix L, Ringgaard S, Sørensen T S and Poulsen P R 2014 Three-dimensional liver motion tracking using real-time two-dimensional MRI *Med. Phys.* **41** 042302
Brynolfsson P, Axelsson J, Holmberg A, Jonsson J H, Goldhaber D, Jian Y, Illerstam F, Engström M, Zackrisson B and Nyholm T 2018 Adapting a GE SIGNA PET/MR scanner for radiotherapy *Med. Phys.* **45** 3546–50
Buerger C, Clough R E, King A P, Schaeffter T and Prieto C 2012 Nonrigid motion modeling of the liver from 3D undersampled self-gated golden-radial phase encoded MRI *IEEE Trans. Med. Imaging* **31** 805–15
Bujold A, Craig T, Jaffray D and Dawson L A 2012 Image-guided radiotherapy: has it influenced patient outcomes? *Seminars in Radiation Oncology* (New York: Elsevier) pp 50–61
Bussels B, Goethals L, Feron M, Bielen D, Dymarkowski S, Suetens P and Haustermans K 2003 Respiration-induced movement of the upper abdominal organs: a pitfall for the three-dimensional conformal radiation treatment of pancreatic cancer *Radiother. Oncol.* **68** 69–74 Cai J, Chang Z, Wang Z, Paul Segars W and Yin F F 2011 Four-dimensional magnetic resonance imaging (4D-MRI) using image-based respiratory surrogate: a feasibility study *Med. Phys.* **38** 6384–94
Cai J, McLawhorn R, Read P W, Larner J M, Yin F F, Benedict S H and Sheng K 2010 Effects of breathing variation on gating window internal target volume in respiratory gated radiation therapy *Med. Phys.* **37** 3927–34
Cai J, Read P W and Sheng K 2008 The effect of respiratory motion variability and tumor size on the accuracy of average intensity projection from four-dimensional computed tomography: an investigation based on dynamic MRI *Med. Phys.* **35** 4974–81
Cai J, Read P W, Altes T A, Molloy J A, Brookeman J R and Sheng K 2006 Evaluation of the reproducibility of lung motion probability distribution function (PDF) using dynamic MRI *Phys. Med. Biol.* **52** 365
Caillet V, Booth J T and Keall P 2017 IGRT and motion management during lung SBRT delivery *Phys. Med.* **44** 113–22
Celicanin Z, Bieri O, Preiswerk F, Cattin P, Scheffler K and Santini F 2015 Simultaneous acquisition of image and navigator slices using CAIPIRINHA for 4D MRI *Magn. Reson. Med.* **73** 669–76
Cervino L I, Du J and Jiang S B 2011 MRI-guided tumor tracking in lung cancer radiotherapy *Phys. Med. Biol.* **56** 3773
Chang J Y, Zhang X, Knopf A, Li H, Mori S, Dong L, Lu H-M, Liu W, Badiyan S N and Both S 2017 Consensus guidelines for implementing pencil beam scanning proton therapy for thoracic malignancies on behalf of PTCOG thoracic and lymphoma subcommittee *Int. J. Radiat. Oncol. Biol. Phys.* **99** 41–50
Connell P P and Hellman S 2009 Advances in radiotherapy and implications for the next century: a historical perspective *Cancer Res.* **69** 383–92
Crijns S, Kok J, Lagendijk J and Raaymakers B 2011 Towards MRI-guided linear accelerator control: gating on an MRI accelerator *Phys. Med. Biol.* **56** 4815
Daniel M, Andrzejewski P, Sturdza A, Majercakova K, Baltzer P, Pinker K, Wadsak W, Mitterhauser M, Pötter R and Georg P 2017 Impact of hybrid PET/MR technology on multiparametric imaging and treatment response assessment of cervix cancer *Radiother. Oncol.* **125** 420–5
Dawson L A and Sharpe M B 2006 Image-guided radiotherapy: rationale, benefits, and limitations *Lancet Oncol.* **7** 848–58
de la Zerda A, Armbruster B and Xing L 2007 Formulating adaptive radiation therapy (ART) treatment planning into a closed-loop control framework *Phys. Med. Biol.* **52** 4137
Deng Z, Pang J, Yang W, Yue Y, Sharif B, Tuli R, Li D, Fraass B and Fan Z 2016 4D MRI using 3D radial sampling with respiratory self-gating to characterize temporal phase-resolved respiratory motion in the abdomen *Magn. Reson. Med.* **75** 1574
Dhont J, Vandemeulebroucke J, Burghelea M, Poels K, Depuydt T, Van Den Begin R, Jaudet C, Collen C, Engels B and Reynders T 2018 The long-and short-term variability of breathing induced tumor motion in lung and liver over the course of a radiotherapy treatment *Radiother. Oncol.* **126** 339–46
Dinkel J, Hintze C, Tetzlaff R, Huber P E, Herfarth K, Debus J, Kauczor H U and Thieke C 2009 4D-MRI analysis of lung tumor motion in patients with hemidiaphragmatic paralysis *Radiother. Oncol.* **91** 449–54
Dowling J, Dang K, Fox C D, Chandra S, Gill S, Kron T, Pham D and Foroudi F 2014 Fast cine-magnetic resonance imaging point tracking for prostate cancer radiation therapy planning *J. Phys.: Conf. Ser.* **489** 012027
Du D, Caruthers S D, Glide-Hurst C, Low D A, Li H H, Mutic S and Hu Y 2015 High-quality T2-weighted 4-dimensional magnetic resonance imaging for radiation therapy applications *Int. J. Radiat. Oncol. Biol. Phys.* **92** 430–7
Edmund J M and Nyholm T 2017 A review of substitute CT generation for MRI-only radiation therapy *Radiat. Oncol.* **12** 28
Ehrbar S, Jöhl A, Tartas A, Stark L S, Riesterer O, Klöck S, Guckenberger M and Tanadini-Lang S 2017 ITV, mid-ventilation, gating or couch tracking–a comparison of respiratory motion-management techniques based on 4D dose calculations *Radiother. Oncol.* **124** 80–8 Fallone B G 2014 The rotating biplanar linac–magnetic resonance imaging system *Seminars in Radiation Oncology* (New York: Elsevier) pp 200–2
Fast M F, Eiben B, Menten M J, Wetscherek A, Hawkes D J, McClelland J R and Oelfke U 2017 Tumour auto-contouring on 2d cine MRI for locally advanced lung cancer: a comparative study *Radiother. Oncol.* **125** 485–91
Fayad H J, Buerger C, Tsoumpas C, Cheze-Le-Rest C and Visvikis D 2012 A generic respiratory motion model based on 4D MRI imaging and 2D image navigators *2012 IEEE Nuclear Science Symp. and Medical Imaging Conf. (NSS/MIC)* (IEEE) pp 4058–61
Fayad H, Schmidt H, Küstner T and Visvikis D 2017 4-dimensional MRI and attenuation map generation in PET/MRI with 4-dimensional PET-derived deformation matrices: study of feasibility for lung cancer applications *J. Nucl. Med.* **58** 833–9
Feng L, Axel L, Chandarana H, Block K T, Sodickson D K and Otazo R 2016 XD-GRASP: golden-angle radial MRI with reconstruction of extra motion-state dimensions using compressed sensing *Magn. Reson. Med.* **75** 775–88
Feng L, Grimm R, Block K T, Chandarana H, Kim S, Xu J, Axel L, Sodickson D K and Otazo R 2014 Golden-angle radial sparse parallel MRI: combination of compressed sensing, parallel imaging, and golden-angle radial sampling for fast and flexible dynamic volumetric MRI *Magn. Reson. Med.* **72** 707–17
Feng M, Balter J M, Normolle D, Adusumilli S, Cao Y, Chenevert T L and Ben-Josef E 2009 Characterization of pancreatic tumor motion using cine MRI: surrogates for tumor position should be used with caution *Int. J. Radiat. Oncol. Biol. Phys.* **74** 884–91
Fernandes T A, Apisarnthanarax S, Yin L, Zou W, Rosen M, Plastaras J P, Ben-Josef E, Metz J M and Teo B-K 2015 Comparative assessment of liver tumor motion using cine-magnetic resonance imaging versus 4-dimensional computed tomography *Int. J. Radiat. Oncol. Biol. Phys.* **91** 1034–40

Fontana G, Riboldi M, Gianoli C, Chirvase C I, Villa G, Paganelli C, Summers P E, Tagaste B, Pella A and Fossati P 2016 MRI quantification of pancreas motion as a function of patient setup for particle therapy—a preliminary study *J. Appl. Clin. Med. Phys.* **17** 60–75

Ge J, Santanam L, Noel C and Parikh P J 2013 Planning 4-dimensional computed tomography (4D CT) cannot adequately represent daily intrafractional motion of abdominal tumors *Int. J. Radiat. Oncol. Biol. Phys.* **85** 999–1005

Glitzner M, Crijns S, De Senneville B D, Kontaxis C, Prins F, Lagendijk J and Raaymakers B 2015a On-line MR imaging for dose validation of abdominal radiotherapy *Phys. Med. Biol.* **60** 8869

Glitzner M, Crijns S, de Senneville B D, Lagendijk J and Raaymakers B 2015b On the suitability of Elekta's agility 160 MLC for tracked radiation delivery: closed-loop machine performance *Phys. Med. Biol.* **60** 2005–17

Gou S, Wu J, Liu F, Lee P, Rapacchi S, Hu P and Sheng K 2014 Feasibility of automated pancreas segmentation based on dynamic MRI *Br. J. Radiol.* **87** 20140248

Griswold M A, Jakob P M, Heidemann R M, Nittka M, Jellus V, Wang J, Kiefer B and Haase A 2002 Generalized autocalibrating partially parallel acquisitions (GRAPPA) *Magn. Reson. Med.* **47** 1202–10

Harris W, Ren L, Cai J, Zhang Y, Chang Z and Yin F-F 2016 A technique for generating volumetric cine-magnetic resonance imaging *Int. J. Radiat. Oncol. Biol. Phys.* **95** 844–53

Hartman J, Kontaxis C, Bol G, Frank S, Lagendijk J, van Vulpen M and Raaymakers B 2015 Dosimetric feasibility of intensity modulated proton therapy in a transverse magnetic field of 1.5 T *Phys. Med. Biol.* **60** 5955

Heerkens H D, van Vulpen M, van den Berg C A, Tijssen R H, Crijns S P, Molenaar I Q, van Santvoort H C, Reerink O and Meijer G J 2014 MRI-based tumor motion characterization and gating schemes for radiation therapy of pancreatic cancer *Radiother. Oncol.* **111** 252–7

Heidemann R M, Özsarlak Ö, Parizel P M, Michiels J, Kiefer B, Jellus V, Müller M, Breuer F, Blaimer M and Griswold M A 2003 A brief review of parallel magnetic resonance imaging *Eur. Radiol.* **13** 2323–37

Henke L, Kashani R, Robinson C, Curcuru A, DeWees T, Bradley J, Green O, Michalski J, Mutic S and Parikh P 2018 Phase I trial of stereotactic MR-guided online adaptive radiation therapy (SMART) for the treatment of oligometastatic or unresectable primary malignancies of the abdomen *Radiother. Oncol.* **126** 519–26

Hoover D A, Capaldi D P, Sheikh K, Palma D A, Rodrigues G B, Dar A R, Yu E, Dingle B, Landis M and Kocha W 2014 Functional lung avoidance for individualized radiotherapy (FLAIR): study protocol for a randomized, double-blind clinical trial *BMC Cancer* **14** 934 Høyer M, Thor M, Thörnqvist S, Søndergaard J, Lassen-Ramshad Y and Muren L P 2011 Advances in radiotherapy: from 2D to 4D *Cancer Imaging* **11** S147

Hu Y, Caruthers S D, Low D A, Parikh P J and Mutic S 2013 Respiratory amplitude guided 4-dimensional magnetic resonance imaging *Int. J. Radiat. Oncol. Biol. Phys.* **86** 198–204

Hugo G D and Rosu M 2012 Advances in 4D radiation therapy for managing respiration: part I–4D imaging *Z. Med. Phys.* **22** 258–71

Hui C, Wen Z, Stemkens B, Tijssen R, Van Den Berg C, Hwang K-P and Beddar S 2016 4D MR imaging using robust internal respiratory signal *Phys. Med. Biol.* **61** 3472

Hunt A, Hansen V, Oelfke U, Nill S and Hafeez S 2018 Adaptive radiotherapy enabled by MRI guidance *Clin. Oncol.*

ICRU 1999 *Prescribing, Recording and Reporting Photon Beam Therapy* (*International Commission on Radiation Units and Measurements: ICRU Report 62*) *Journal of the International Commission on Radiation Units and Measurements* **os32**

Jaffray D A 2012 Image-guided radiotherapy: from current concept to future perspectives *Nat. Rev. Clin. Oncol.* **9** 688–99

Jaffray D A, Carlone M C, Milosevic M F, Breen S L, Stanescu T, Rink A, Alasti H, Simeonov A, Sweitzer M C and Winter J D 2014 A facility for magnetic resonance-guided radiation therapy *Seminars in Radiation Oncology* (New York: Elsevier) pp 193–5

Jiang N, Cao M, Lamb J, Sheng K, Mikaeilian A, Low D, Raldow A, Steinberg M and Lee P 2017a Outcomes utilizing MRI-guided and real-time adaptive pancreas stereotactic body radiotherapy (SBRT) *Int. J. Radiat. Oncol. Biol. Phys.* **99** S146

Jiang W, Ong F, Johnson K M, Nagle S K, Hope T A, Lustig M and Larson P E 2017b Motion robust high resolution 3D free-breathing pulmonary MRI using dynamic 3D image self-navigator *Magn. Reson. Med.* **79** 2954–67

Johnstone E, Wyatt J J, Henry A M, Short S C, Sebag-Montefiore D, Murray L, Kelly C G, McCallum H M and Speight R 2017 A systematic review of synthetic CT generation methodologies for use in MRI-only radiotherapy *Int. J. Radiat. Oncol. Biol. Phys.* **100** 199–217

Jonsson J H, Karlsson M G, Karlsson M and Nyholm T 2010 Treatment planning using MRI data: an analysis of the dose calculation accuracy for different treatment regions *Radiat. Oncol.* **5** 62

Karlsson M, Karlsson M G, Nyholm T, Amies C and Zackrisson B 2009 Dedicated magnetic resonance imaging in the radiotherapy clinic *Int. J. Radiat. Oncol. Biol. Phys.* **74** 644–51

Kashani R and Olsen J R 2018 Magnetic resonance imaging for target delineation and daily treatment modification *Seminars in Radiation Oncology* (New York: Elsevier) pp 178–84

Kauczor H-U and Plathow C 2006 Imaging tumour motion for radiotherapy planning using MRI *Cancer Imaging* **6** S140

Kauczor H-U, Zechmann C, Stieltjes B and Weber M-A 2006 Functional magnetic resonance imaging for defining the biological target volume *Cancer Imaging* **6** 51–5

Keall P J, Barton M and Crozier S 2014 The Australian magnetic resonance imaging-linac program *Seminars in Radiation Oncology* (New York: Elsevier) pp 203–06

Keall P J, Mageras G S, Balter J M, Emery R S, Forster K M, Jiang S B, Kapatoes J M, Low D A, Murphy M J and Murray B R 2006 The management of respiratory motion in radiation oncology report of AAPM Task Group 76 *Med. Phys.* **33** 3874–900

Kerkhof E, Balter J, Vineberg K and Raaymakers B 2010 Treatment plan adaptation for MRI-guided radiotherapy using solely MRI data: a CT-based simulation study *Phys. Med. Biol.* **55** N433

Keyvanloo A, Burke B, Warkentin B, Tadic T, Rathee S, Kirkby C, Santos D and Fallone B 2012 Skin dose in longitudinal and transverse linac-MRIs using Monte Carlo and realistic 3D MRI field models *Med. Phys.* **39** 6509–21

Kim T, Pollock S, Lee D, O'Brien R and Keall P 2012 Audiovisual biofeedback improves diaphragm motion reproducibility in MRI *Med. Phys.* **39** 6921–8

Kirilova A, Lockwood G, Choi P, Bana N, Haider M A, Brock K K, Eccles C and Dawson L A 2008 Three-dimensional motion of liver tumors using cine-magnetic resonance imaging *Int. J. Radiat. Oncol. Biol. Phys.* **71** 1189–95

Koch N, Liu H H, Starkschall G, Jacobson M, Forster K, Liao Z, Komaki R and Stevens C W 2004 Evaluation of internal lung motion for respiratory-gated radiotherapy using MRI: part I—correlating internal lung motion with skin fiducial motion *Int. J. Radiat. Oncol. Biol. Phys.* **60** 1459–72

Kontaxis C, Bol G, Lagendijk J and Raaymakers B 2015a A new methodology for inter-and intrafraction plan adaptation for the MR-linac *Phys. Med. Biol.* **60** 7485

Kontaxis C, Bol G, Lagendijk J and Raaymakers B 2015b Towards adaptive IMRT sequencing for the MR-linac *Phys. Med. Biol.* **60** 2493

Kontaxis C, Bol G, Stemkens B, Glitzner M, Prins F, Kerkmeijer L, Lagendijk J and Raaymakers B 2017 Towards fast online intrafraction replanning for free-breathing stereotactic body radiation therapy with the MR-linac *Phys. Med. Biol.* **62** 7233

Korreman S S 2012 Motion in radiotherapy: photon therapy *Phys. Med. Biol.* **57** R161

Krauss A, Nill S and Oelfke U 2011 The comparative performance of four respiratory motion predictors for real-time tumour tracking *Phys. Med. Biol.* **56** 5303

Kubiak T 2016 Particle therapy of moving targets—the strategies for tumour motion monitoring and moving targets irradiation *Br. J. Radiol.* **89** 20150275

Kurz C, Landry G, Resch A F, Dedes G, Kamp F, Ganswindt U, Belka C, Raaymakers B W and Parodi K 2017 A Monte-Carlo study to assess the effect of 1.5 T magnetic fields on the overall robustness of pencil-beam scanning proton radiotherapy plans for prostate cancer *Phys. Med. Biol.* **62** 8470

Küstner T, Würslin C, Schwartz M, Martirosian P, Gatidis S, Brendle C, Seith F, Schick F, Schwenzer N F and Yang B 2017 Self-navigated 4D cartesian imaging of periodic motion in the body trunk using partial k-space compressed sensing *Magn. Reson. Med.* **78** 632–44

Lagendijk J J, Raaymakers B W, Van den Berg C A, Moerland M A, Philippens M E and Van Vulpen M 2014 MR guidance in radiotherapy *Phys. Med. Biol.* **59** R349

Lee D, Greer P B, Ludbrook J, Arm J, Hunter P, Pollock S, Makhija K, O'brien R T, Kim T and Keall P 2016 Audiovisual biofeedback improves cine-magnetic resonance imaging measured lung tumor motion consistency *Int. J. Radiat. Oncol. Biol. Phys.* **94** 628–36

Lens E, van der Horst A, Versteijne E, van Tienhoven G and Bel A 2015 Dosimetric advantages of midventilation compared with internal target volume for radiation therapy of pancreatic cancer *Int. J. Radiat. Oncol. Biol. Phys.* **92** 675–82

Li G, Wei J, Olek D, Kadbi M, Tyagi N, Zakian K, Mechalakos J, Deasy J O and Hunt M 2016 Direct comparison of respiration-correlated four-dimensional magnetic resonance imaging reconstructed using concurrent internal navigator and external bellows *Int. J. Radiat. Oncol. Biol. Phys.* **97** 596–605

Li G, Wei J, Olek D, Kadbi M, Tyagi N, Zakian K, Mechalakos J, Deasy J O and Hunt M 2017 Direct comparison of respiration-correlated four-dimensional magnetic resonance imaging reconstructed using concurrent internal navigator and external bellows *Int. J. Radiat. Oncol. Biol. Phys.* **97** 596–605

Li J G and Xing L 2000 Inverse planning incorporating organ motion *Med. Phys.* **27** 1573–8

Liang X, Yin F F, Liu Y and Cai J 2016 A probability-based multi-cycle sorting method for 4D-MRI: A simulation study *Med. Phys.* **43** 6375–85

Liu H H, Koch N, Starkschall G, Jacobson M, Forster K, Liao Z, Komaki R and Stevens C W 2004 Evaluation of internal lung motion for respiratory-gated radiotherapy using MRI: part II—margin reduction of internal target volume *Int. J. Radiat. Oncol. Biol. Phys.* **60** 1473–83

Liu Y, Yin F F, Chang Z, Czito B G, Palta M, Bashir M R, Qin Y and Cai J 2014 Investigation of sagittal image acquisition for 4D-MRI with body area as respiratory surrogate *Med. Phys.* **41** 101902

Liu Y, Yin F F, Czito B G, Bashir M R and Cai J 2015 T2-weighted four dimensional magnetic resonance imaging with result-driven phase sorting *Med. Phys.* **42** 4460–71

Liu Y, Yin F F, Rhee D and Cai J 2016a Accuracy of respiratory motion measurement of 4D-MRI: A comparison between cine and sequential acquisition *Med. Phys.* **43** 179–87

Liu Y, Yin F-F, Czito B G, Bashir M R, Palta M and Cai J 2017 Retrospective four-dimensional magnetic resonance imaging with image-based respiratory surrogate: a sagittal–coronal–diaphragm point of intersection motion tracking method *J. Med. Imaging* **4** 024007

Liu Y, Zhong X, Czito B G, Palta M, Bashir M R, Dale B M, Yin F F and Cai J 2016b Four-dimensional diffusion-weighted MR imaging (4D-DWI): a feasibility study *Med. Phys.* **44** 397–406

Lustig M, Donoho D L, Santos J M and Pauly J M 2008 Compressed sensing MRI *IEEE Signal Process. Mag.* **25** 72–82

Marx M, Ehrhardt J, Werner R, Schlemmer H-P and Handels H 2014 Simulation of spatiotemporal CT data sets using a 4D MRI-based lung motion model *Int. J. Comput. Assist. Radiol. Surg.* **9** 401–9

Maspero M, Van den Berg C A, Landry G, Belka C, Parodi K, Seevinck P R, Raaymakers B W and Kurz C 2017 Feasibility of MR-only proton ose calculations for prostate cancer radiotherapy using a commercial pseudo-CT generation method *Phys. Med. Biol.* **62** 9159 Mazur T R, ischer-Valuck B W, Wang Y, Yang D, Mutic S and Li H H 2016 SIFT-based dense pixel tracking on 0.35 T cine-MR images acquired during image-guided radiation therapy with application to gating optimization *Med. Phys.* **43** 279–93

McClelland J R *et al* 2017 A generalized framework unifying image registration and respiratory motion models and incorporating image reconstruction, for partial image data or full images *Phys. Med. Biol.* **62** 4273–92

McClelland J R, Hawkes D J, Schaeffter T and King A P 2013 Respiratory motion models: a review *Med. Image Anal.* **17** 19–42

McRobbie D W, Moore E A and Graves M J 2017 *MRI from Picture to Proton* (Cambridge: Cambridge University Press)

Ménard C and van der Heide U 2014 Introduction: systems for magnetic resonance image guided radiation therapy *Seminars in Radiation Oncology* (New York: Elsevier) p 192

Menten M J, Wetscherek A and Fast M F 2017 MRI-guided lung SBRT: Present and future developments *Phys. Med.* **139** 139–49

Mickevicius N J and Paulson E S 2017a Investigation of undersampling and reconstruction algorithm dependence on respiratory correlated 4D-MRI for online MR-guided radiation therapy *Phys. Med. Biol.* **62** 2910

Mickevicius N J and Paulson E S 2017b Simultaneous orthogonal plane imaging *Magn. Reson. Med.* **78** 1700–10

Mutic S and Dempsey J F 2014 The ViewRay system: magnetic resonance-guided and controlled radiotherapy *Seminars in Radiation Oncology* (New York: Elsevier) pp 196–9

Oborn B M, Dowdell S, Metcalfe P E, Crozier S, Mohan R and Keall P J 2017 Future of medical physics: real-time MRI guided proton therapy *Med. Phys.* **44** e77–90

Oborn B M, Ge Y, Hardcastle N, Metcalfe P E and Keall P J 2016 Dose enhancement in radiotherapy of small lung tumors using inline magnetic fields: a Monte Carlo based planning study *Med. Phys.* **43** 368–77

Oborn B, Kolling S, Metcalfe P E, Crozier S, Litzenberg D and Keall P 2014 Electron contamination modeling and reduction in a 1 T open bore inline MRI-linac system *Med. Phys.* **41**

Odille F, Vuissoz P-A, Marie P-Y and Felblinger J 2008 Generalized reconstruction by inversion of coupled systems (GRICS) applied to free-breathing MRI *Magn. Reson. Med.* **60** 146–57

Olsen J, Green O and Kashani R 2014 World's first application of MR-guidance for radiotherapy *Missouri Med.* **112** 358–60

Paganelli C, Kipritidis J, Lee D, Baroni G, Keall P and Riboldi M 2018 Image-based retrospective 4D MRI in external beam radiotherapy: a comparative study with a digital phantom *Med Phys.* **45** 3161–72

Paganelli C, Lee D, Greer P B, Baroni G, Riboldi M and Keall P 2015a Quantification of lung tumor rotation with automated landmark extraction using orthogonal cine MRI images *Phys. Med. Biol.* **60** 7165

Paganelli C, Seregni M, Fattori G, Summers P, Bellomi M, Baroni G and Riboldi M 2015b Magnetic resonance imaging-guided versus surrogate-based motion tracking in liver radiation therapy: a prospective comparative study *Int. J. Radiat. Oncol. Biol. Phys.* **91** 840–8

Paganelli C, Summers P, Bellomi M, Baroni G and Riboldi M 2015c Liver 4D MRI: a retrospective image-based sorting method *Med. Phys.* **42** 4814–21

Park S, Farah R, Shea S M, Tryggestad E, Hales R and Lee J 2018 Simultaneous tumor and surrogate motion tracking with dynamic MRI for radiation therapy planning *Phys. Med. Biol.* **63** 025015

Plathow C, Klopp M, Fink C, Sandner A, Hof H, Puderbach M, Herth F, Schmähl A and Kauczor H 2005 Quantitative analysis of lung and tumour mobility: comparison of two time-resolved MRI sequences *Br. J. Radiol.* **78** 836–40

Plathow C, Ley S, Fink C, Puderbach M, Hosch W, Schmähl A, Debus J and Kauczor H-U 2004 Analysis of intrathoracic tumor mobility during whole breathing cycle by dynamic MRI *Int. J. Radiat. Oncol. Biol. Phys.* **59** 952–9

Plathow C, Schoebinger M, Fink C, Hof H Jr, Debus J, Meinzer H-P and Kauczor H-U 2006 Quantification of lung tumor volume and rotation at 3D dynamic parallel MR imaging with view sharing: preliminary results 1 *Radiology* **240** 537–45

Plathow C, Schoebinger M, Herth F, Tuengerthal S, Meinzer H-P and Kauczor H-U 2009 Estimation of pulmonary motion in healthy subjects and patients with intrathoracic tumors using 3D-dynamic MRI: initial results *Korean J. Radiol.* **10** 559–67

Prestwich R, Vaidyanathan S and Scarsbrook A 2015 Functional imaging biomarkers: potential to guide an individualised approach to radiotherapy *Clin. Oncol.* **27** 588–600

Pruessmann K P 2006 Encoding and reconstruction in parallel MRI *NMR Biomed.* **19** 288–99

Raaijmakers A, Hårdemark B, Raaymakers B, Raaijmakers C and Lagendijk J 2007 Dose optimization for the MRI-accelerator: IMRT in the presence of a magnetic field *Phys. Med. Biol.* **52** 7045

Raaymakers B, Jürgenliemk-Schulz I, Bol G, Glitzner M, Kotte A, van Asselen B, de Boer J, Bluemink J, Hackett S and Moerland M 2017 First patients treated with a 1.5 T MRI-Linac: clinical proof of concept of a high-precision, high-field MRI guided radiotherapy treatment *Phys. Med. Biol.* **62** L41

Rank C M, Heußer T, Buzan M T, Wetscherek A, Freitag M T, Dinkel J and Kachelrieß M 2017 4D respiratory motion-compensated image reconstruction of free-breathing radial MR data with very high undersampling *Magn. Reson. Med.* **77** 1170–83

Rank C M, Heußer T, Wetscherek A, Freitag M T, Sedlaczek O, Schlemmer H P and Kachelrieß M 2016 Respiratory motion compensation for simultaneous PET/MR based on highly undersampled MR data *Med. Phys.* **43** 6234–45

Riboldi M, Orecchia R and Baroni G 2012 Real-time tumour tracking in particle therapy: technological developments and future perspectives *Lancet Oncol.* **13** e383–91

Rohlfing T, Maurer C R, O' Dell W G and Zhong J 2004 Modeling liver motion and deformation during the respiratory cycle using intensity-based nonrigid registration of gated MR images *Med. Phys.* **31** 427–32

Rosenblatt E and Zubizarreta E 2017 *Radiotherapy in Cancer Care: Facing the Global Challenge* (Vienna, Austria: International Atomic Energy Agency)

Rosu M and Hugo G D 2012 Advances in 4D radiation therapy for managing respiration: part II–4D treatment planning *Z. Med. Phys.* **22** 272–80

Ruan D, Fessler J A, Balter J, Berbeco R, Nishioka S and Shirato H 2008 Inference of hysteretic respiratory tumor motion from external surrogates: a state augmentation approach *Phys. Med. Biol.* **53** 2923

Ruschin M, Sahgal A, Tseng C-L, Sonier M, Keller B and Lee Y 2017 Dosimetric impact of using a virtual couch shift for online correction of setup errors for brain patients on an integrated high-field magnetic resonance imaging linear accelerator *Int. J. Radiat. Oncol. Biol. Phys.* **98** 699–708

Sawant A, Keall P, Pauly K B, Alley M, Vasanawala S, Loo B W Jr, Hinkle J and Joshi S 2014 Investigating the feasibility of rapid MRI for image-guided motion management in lung cancer radiotherapy *Biomed. Res. Int.* **2014** 485067

Schmidt M A and Payne G S 2015 Radiotherapy planning using MRI *Phys. Med. Biol.* **60** R323

Schwarz M, Cattaneo G M and Marrazzo L 2017 Geometrical and dosimetrical uncertainties in hypofractionated radiotherapy of the lung: a review *Phys. Med.* **36** 126–39

Seregni M, Paganelli C, Lee D, Greer P, Baroni G, Keall P and Riboldi M 2016 Motion prediction in MRI-guided radiotherapy based on interleaved orthogonal cine-MRI *Phys. Med. Biol.* **61** 872

Seregni M, Paganelli C, Summers P, Bellomi M, Baroni G and Riboldi M 2017 A hybrid image registration and matching framework for real-time motion tracking in MRI-guided radiotherapy *IEEE Trans. Biomed. Eng.* **65** 131–9

Shi X, Diwanji T, Mooney K E, Lin J, Feigenberg S, D' Souza W D and Mistry N N 2014 Evaluation of template matching for tumor motion management with cine-MR images in lung cancer patients *Med. Phys.* **41** 052304

Simpson D R, Lawson J D, Nath S K, Rose B S, Mundt A J and Mell L K 2009 Utilization of advanced imaging technologies for target delineation in radiation oncology *J. Am. College Radiol.* **6** 876–83

Song R, Tipirneni A, Johnson P, Loeffler R B and Hillenbrand C M 2011 Evaluation of respiratory liver and kidney movements for MRI navigator gating *J. Magn. Reson. Imaging* **33** 143–8

Stam M K, Van Vulpen M, Barendrecht M M, Zonnenberg B A, Crijns S P, Lagendijk J J and Raaymakers B W 2013a Dosimetric feasibility of MRI-guided external beam radiotherapy of the kidney *Phys. Med. Biol.* **58** 4933

Stam M K, Van Vulpen M, Barendrecht M M, Zonnenberg B A, Intven M, Crijns S P, Lagendijk J J and Raaymakers B W 2013b Kidney motion during free breathing and breath hold for MR-guided radiotherapy *Phys. Med. Biol.* **58** 2235

Stemkens B, Glitzner M, Kontaxis C, De Senneville B D, Prins F M, Crijns S P, Kerkmeijer L G, Lagendijk J J, Van Den Berg C A and Tijssen R H 2017 Effect of intra-fraction motion on the accumulated dose for free-breathing MR-guided stereotactic body radiation therapy of renal-cell carcinoma *Phys. Med. Biol.* **62** 7407

Stemkens B, Tijssen R H, de Senneville B D, Heerkens H D, van Vulpen M, Lagendijk J J and van den Berg C A 2015 Optimizing 4-dimensional magnetic resonance imaging data sampling for respiratory motion analysis of pancreatic tumors *Int. J. Radiat. Oncol. Biol. Phys.* **91** 571–8

Stemkens B, Tijssen R H, de Senneville B D, Lagendijk J J and van den Berg C A 2016 Image-driven, model-based 3D abdominal motion estimation for MR-guided radiotherapy *Phys. Med. Biol.* **61** 5335

Thomas D H, Santhanam A, Kishan A U, Cao M, Lamb J, Min Y, O' Connell D, Yang Y, Agazaryan N and Lee P 2017 Initial observations of intra-and inter-fractional motion variation in MR guided lung SBRT *Br. J. Radiol.* **1083** 20170522

To D T, Kim J P, Price R G, Chetty I J and Glide-Hurst C K 2016 Impact of incorporating visual biofeedback in 4D MRI *J. Appl. Clin. Med. Phys.* **17** 128–37

Tokuda J, Morikawa S, Haque H A, Tsukamoto T, Matsumiya K, Liao H, Masamune K and Dohi T 2008 Adaptive 4D MR imaging using navigator-based respiratory signal for MRI-guided therapy *Magn. Reson. Med.* **59** 1051–61

Torfeh T, Hammoud R, El Kaissi T, McGarry M, Aouadi S, Fayad H and Al-Hammadi N 2018 Geometric accuracy of the MR imaging techniques in the presence of motion *J. Appl. Clin. Med. Phys.* **19** 168–75
Tryggestad E, Flammang A, Hales R, Herman J, Lee J, McNutt T, Roland T, Shea S M and Wong J 2013a 4D tumor centroid tracking using orthogonal 2D dynamic MRI: implications for radiotherapy planning *Med. Phys.* **40** 091712
Tryggestad E, Flammang A, Han-Oh S, Hales R, Herman J, McNutt T, Roland T, Shea S M and Wong J 2013b Respiration-based sorting of dynamic MRI to derive representative 4D-MRI for radiotherapy planning *Med. Phys.* **40** 051909
Uh J, Khan M A and Hua C 2016 Four-dimensional MRI using an internal respiratory surrogate derived by dimensionality reduction *Phys. Med. Biol.* **61** 7812
Unkelbach J and Oelfke U 2004 Inclusion of organ movements in IMRT treatment planning via inverse planning based on probability distributions *Phys. Med. Biol.* **49** 4005
van de Lindt T N, Fast M F, van der Heide U A and Sonke J-J 2018b Retrospective self-sorted 4D-MRI for the liver *Radiother. Oncol.* **127** 474–80
van de Lindt T N, Schubert G, van der Heide U A and Sonke J-J 2016 An MRI-based mid-ventilation approach for radiotherapy of the liver *Radiother. Oncol.* **121** 276–80
van de Lindt T, Sonke J-J, Nowee M, Jansen E, van Pelt V, van der Heide U and Fast M 2018a A self-sorting coronal 4D-MRI method for daily image guidance of liver lesions on an MR-linac *Int. J. Radiat. Oncol. Biol. Phys.* **102** 875–884
van der Heide U A, Houweling A C, Groenendaal G, Beets-Tan R G and Lambin P 2012 Functional MRI for radiotherapy dose painting *Magn. Reson. Imaging* **30** 1216–23
Van Heijst T C, Philippens M E, Charaghvandi R K, Den Hartogh M D, Lagendijk J J, van den Bongard H D and van Asselen B 2016 Quantification of intra-fraction motion in breast radiotherapy using supine magnetic resonance imaging *Phys. Med. Biol.* **61** 1352
Van Herk M 2004 Errors and margins in radiotherapy *Seminars in Radiation Oncology* (New York: Elsevier) pp 52–64
Varoquaux A, Rager O, Dulguerov P, Burkhardt K, Ailianou A and Becker M 2015 Diffusion-weighted and PET/MR imaging after radiation therapy for malignant head and neck tumors *Radiographics* **35** 1502–27
Venselaar J, Welleweerd H and Mijnheer B 2001 Tolerances for the accuracy of photon beam dose calculations of treatment planning systems *Radiother. Oncol.* **60** 191–201
Verellen D, De Ridder M and Storme G 2008 A (short) history of image-guided radiotherapy *Radiother. Oncol.* **86** 4–13
Von Siebenthal M, Székely G, Gamper U, Boesiger P, Lomax A and Cattin P 2007 4D MR imaging of respiratory organ motion and its variability *Phys. Med. Biol.* **52** 1547
Wachinger C, Yigitsoy M, Rijkhorst E-J and Navab N 2012 Manifold learning for image-based breathing gating in ultrasound and MRI *Med. Image Anal.* **16** 806–18
Weick S, Völker M, Hemberger K, Meyer C, Ehses P, Polat B, Breuer F A, Blaimer M, Fink C and Schad L R 2017 Desynchronization of Cartesian *k*-space sampling and periodic motion for improved retrospectively self-gated 3D lung MRI using quasi-random numbers *Magn. Reson. Med.* **77** 787–93
Weiss J, Notohamiprodjo M, Martirosian P, Taron J, Nickel M D, Kolb M, Bamberg F, Nikolaou K and Othman A E 2017 Self-gated 4D-MRI of the liver: initial clinical results of continuous multiphase imaging of hepatic enhancement *J. Magn. Reson. Imaging* **47** 459–467
Whelan B, Liney G P, Dowling J A, Rai R, Holloway L, McGarvie L, Feain I, Barton M, Berry M and Wilkins R 2017 An MRI-compatible patient rotation system—design, construction, and first organ deformation results *Med. Phys.* **44** 581–8
Wojcieszynski A P, Rosenberg S A, Brower J V, Hullett C R, Geurts M W, Labby Z E, Hill P M, Bayliss R A, Paliwal B and Bayouth J E 2016 Gadoxetate for direct tumor therapy and tracking with real-time MRI-guided stereotactic body radiation therapy of the liver *Radiother. Oncol.* **118** 416–8
Wolthaus J W, Schneider C, Sonke J-J, van Herk M, Belderbos J S, Rossi M M, Lebesque J V and Damen E M 2006 Mid-ventilation CT scan construction from four-dimensional respiration-correlated CT scans for radiotherapy planning of lung cancer patients *Int. J. Radiat. Oncol. Biol. Phys.* **65** 1560–71
Wolthaus J W, Sonke J-J, van Herk M, Belderbos J S, Rossi M M, Lebesque J V and Damen E M 2008 Comparison of different strategies to use four-dimensional computed tomography in treatment planning for lung cancer patients *Int. J. Radiat. Oncol. Biol. Phys.* **70** 1229–38 Yang Y, Cao M, Sheng K, Gao Y, Chen A, Kamrava M, Lee P, Agazaryan N, Lamb J and Thomas D 2016 Longitudinal diffusion MRI for treatment response assessment: preliminary experience using an MRI-guided tri-cobalt 60 radiotherapy system *Med. Phys.* **43** 1369–73
Yun J, Mackenzie M, Rathee S, Robinson D and Fallone B 2012 An artificial neural network (ANN)-based lung-tumor motion predictor for intrafractional MR tumor tracking *Med. Phys.* **39** 4423–33
Yun J, Yip E, Gabos Z, Wachowicz K, Rathee S and Fallone B G 2015 Neural-network based autocontouring algorithm for intrafractional lung-tumor tracking using linac-MR *Med. Phys.* **42** 2296–310
Zachiu C, Papadakis N, Ries M, Moonen C and de Senneville B D 2015 An improved optical flow tracking technique for real-time MR-guided beam therapies in moving organs *Phys. Med. Biol.* **60** 9003
Zhang Y, Huth I, Wegner M, Weber D C and Lomax A J 2016 An evaluation of rescanning technique for liver tumour treatments using a commercial PBS proton therapy system *Radiother. Oncol.* **121** 281–7
Zhang Y, Knopf A, Tanner C and Lomax A 2014 Online image guided tumour tracking with scanned proton beams: a comprehensive simulation study *Phys. Med. Biol.* **59** 7793
Zucker E J, Cheng J Y, Haldipur A, Carl M and Vasanawala S S 2017 Free-breathing pediatric chest MRI: Performance of self-navigated golden-angle ordered conical ultrashort echo time acquisition *J. Magn. Reson. Imaging* **47** 200–9